2007

Causing and curing infantile esotropia in primates: The role of decorrelated binocular input (an American Ophthalmological Society thesis)

Lawrence Tychsen
Washington University School of Medicine in St. Louis

CAUSING AND CURING INFANTILE ESOTROPIA IN PRIMATES: THE ROLE OF DECORRELATED BINOCULAR INPUT (AN AMERICAN OPHTHALMOLOGICAL SOCIETY THESIS)

BY Lawrence Tychsen, MD

ABSTRACT

Purpose: Human infants at greatest risk for esotropia are those who suffer cerebral insults that could decorrelate signals from the 2 eyes during an early critical period of binocular, visuomotor development. The author reared normal infant monkeys, under conditions of binocular decorrelation, to determine if this alone was sufficient to cause esotropia and associated behavioral as well as neuroanatomic deficits.

Methods: Binocular decorrelation was imposed using prism-goggles for durations of 3 to 24 weeks (in 6 experimental, 2 control monkeys). Behavioral recordings were obtained, followed by neuroanatomic analysis of ocular dominance columns and binocular, horizontal connections in the striate visual cortex (area V1).

Results: Concomitant, constant esotropia developed in each monkey exposed to decorrelation for a duration of 12 to 24 weeks. The severity of ocular motor signs (esotropia-angle; dissociated vertical deviation; latent nystagmus; pursuit/optokinetic tracking asymmetry; fusional vergence deficits), and the loss of V1 binocular connections, increased as a function of decorrelation duration. Stereopsis was deficient and motion visual evoked potentials were asymmetric. Monkeys exposed to decorrelation for 3 weeks showed transient esotropia but regained normal visuomotor behaviors and binocular V1 connections.

Conclusions: Binocular decorrelation is a sufficient cause of infantile esotropia when imposed during a critical period of visuomotor development. The systematic relationship between severity of visuomotor sign, and severity of V1 connectivity deficit, provides a neuroanatomic mechanism for several of these signs. Restoration of binocular fusion and V1 connections, after short durations of decorrelation, helps explain the benefits of early repair in human strabismus.

Trans Am Ophthalmol Soc 2007;105:564-593

INTRODUCTION

Strabismus (pathologic misalignment of the visual axes) is an important public health problem, depriving 4% to 5% of children of the lifelong advantages bestowed by normal binocular vision.[1-3] The leading form of developmental strabismus is concomitant (nonparalytic) esotropia, which has a bimodal, age-of-onset distribution.[3,4] The largest peak—comprising about 40% of all strabismus—occurs before age 12 months in children who are predominantly emmetropic (the 3- to 4-year-old, "later-onset" age group is predominantly hyperopic). Nonaccommodative, early onset esotropia may be considered the paradigmatic form of strabismus in all primates, as it is also the most frequent type of natural strabismus observed in monkeys.[5]

The cause of infantile-onset esotropia is unknown. Detailed functional and structural studies of the extraocular muscles, orbital connective tissues, and brainstem circuitry in primates with concomitant esotropia have not revealed causal anomalies.[6,7] The striate cortex (area V1) is the first locus in the central nervous system for binocularity,[8,9] and binocular connections in V1 are important for generating the error signals that guide eye alignment.[10-12] Neonates who suffer insults that, directly or indirectly, perturb binocular inputs into V1 have a risk of developing strabismus that is 20 to 100 times higher than that in normal infants.[13-16] These observations led the author to propose a neural mechanism: infantile esotropia could be caused by simply perturbing the development of binocularity in V1, leading downstream, immature motor pathways to decompensate in the direction of innate (nasalward or convergent) biases.

The first goal was to test this hypothesis by rearing neonatal monkeys under conditions that exposed them to periods of sensorial, binocular decorrelation, but left their motor pathways and eye muscles completely intact. The second goal was to determine whether the *duration* of binocular decorrelation predicted the *severity* of any motoric maldevelopment (or the probability of recovery to normal function). These intervals of decorrelation were designed to emulate "early" vs "delayed" strabismus repair in human infants, with the aim of contributing behavioral and neuroanatomic information that could help clarify an issue of clinical controversy.[17-22]

Infantile esotropia in humans is accompanied by a constellation of sensorimotor abnormalities, including deficits of stereopsis and fusional vergence, latent nystagmus, dissociated vertical deviation (DVD), as well as nasotemporal asymmetries of optokinetic tracking, smooth pursuit, and motion visual evoked potentials.[23-26] A good animal model should possess many of the disease features observed in human patients. For this reason, comprehensive behavioral testing was performed to detect (and quantify) these signs. After behavioral testing, binocular connections within area V1 were analyzed using neuroanatomic labeling methods. The goal of the anatomic experiments was to determine if abnormal binocular behaviors were related systematically to abnormal V1 connections.

METHODS

ANIMALS AND GOGGLE REARING GROUPS

Monkeys (*Macaca mulatta*) born at the Yerkes Primate Center in Atlanta, Georgia, were fitted with goggles on the first day of life

From the Departments of Ophthalmology and Visual Sciences, Pediatrics, Anatomy and Neurobiology, Washington University School of Medicine, St Louis, Missouri.

(Figure 1). The fitting procedure was an adaptation of that originally described by Crawford.[27,28] The procedure was not stressful to the newborn macaques and did not require anesthesia or fabrication of a head mold. Padded head straps held the goggles firmly in place and prevented the infant from removing the apparatus, which was custom-fabricated for each monkey from lightweight plastic. The front piece consisted of 2 lens holders, which unscrewed so that ultra-lightweight, 2-mm-thick Fresnel plastic prisms could be inserted. Animals were observed several times per day in the primate nursery and during bottle feedings to ensure that the goggles remained clear and in proper position. The goggles did not interfere noticeably with normal play or mingling with other infant macaques. The goggle helmet was removed from each monkey for cleaning a minimum of once per day. During cleaning and, if necessary, adjustment of the goggle, the animal was placed briefly in a dark (light-tight) enclosure to preclude normal binocular experience. Inspections of the infant monkeys during these brief periods when the goggles were removed for cleaning disclosed that, after several weeks, each of the animals manifested esotropia.

FIGURE 1

Infant monkey wearing prism-goggles to induce binocular image decorrelation.

A total of 8 monkeys were studied: 6 experimental and 2 controls. The 6 experimental monkeys (Table 1) were divided into 3 prism-rearing groups: 3-week (2 animals), 12-week (1 animal), and 24-week (3 animals) groups. In each group, experimental animals wore prism goggles (for periods of 3 to 24 weeks) to impose horizontal and vertical binocular noncorrespondence (decorrelation) of 11.4º (20 prism diopters) in each eye; 11.4º base-in in one eye, and 11.4º base-down in the other eye. The 2 controls wore goggles with plano lenses. At 4 to 6 months of age, the monkeys were shipped to Washington University in St Louis, Missouri, where they were trained to perform visual fixation and tracking tasks without goggles, using a positive-feedback reward (a small bolus of fruit juice).[29] Cycloplegic refractions revealed a refractive error ≤ +3.00 spherical equivalent in each of the experimental and control animals.

At age 1 year, eye coils were implanted29 and ocular motor as well as sensory testing initiated, which proceeded typically for 3 to 6 months. Monocular visual acuity was measured using spatial sweep visual evoked potentials (SSVEP)30,31 (without correction for refractive error).

EYE MOVEMENT RECORDINGS

Detailed descriptions of the surgical and recording methods have been published in previous reports, and for this reason only, an abbreviated description is provided here.[29,32] Using deep general inhalation anesthesia (supplemented by local infiltration and topical anesthesia), scleral search coils were implanted in both eyes and a custom-built, polycarbonate head-restraint device was attached to the skull. All procedures were performed in compliance with the ARVO resolution on the use of animals in research and were approved by the Washington University Animal Care and Use Committee.

Eye movements were recorded using standard magnetic search coil techniques.[33,34] The monkey sat in a primate chair in the middle of field coils. The head restraint was locked to preclude head movement and the room was lit with dim background illumination. Eye position was calibrated at the start of each recording session by using a calibration coil and by having the animal maintain eye position within a 2º window of target position. The target was a laser spot subtending ~ 0.05º projected onto the back of a

translucent screen located 50 cm in front of the animal. The calibration sequence was repeated separately for each eye.

TABLE 1. VISUAL AND OCULAR MOTOR CHARACTERISTICS OF THE 8 MACAQUE MONKEYS IN THE STUDY

ANIMAL/SEX/ AGE IN YEARS (SPECIES)	REARING CONDITIONS	EYE ALIGNMENT AT TESTING	LATENT NYSTAGMUS	PURSUIT/ OKN ASYMMETRY	DVD	VISUAL ACUITY SSVEP (CPD)
3-week Group						
TE/M/1.5	3 weeks prism	Orthophoric	No	No	No	OD: 19.85
(*M mulatta*)	(11.4º BI OD; 11.4º BD OS)					OS: 21.40
SY/M/1.7	3 weeks prism	Orthophoric	No	No	No	OD: 17.95
(*M mulatta*)	(11.4º BI OD; 11.4º BD OS)					OS: 22.80
WE/M/1.5	3 weeks plano (control)	Orthophoric	No	No	No	OD: 22.85
(*M mulatta*)	(0º)					OS: 20.50
12-week Group						
GO/M/2	12 weeks prism	Esotropic	Yes	Yes	Yes	OD: 8.25
(*M mulatta*)	(11.4º BI OD; 11.4º BD OS)					OS: 10.64
AY/M/2	12 weeks plano (control)	Orthophoric	No	No	No	OD: 18.09
(*M mulatta*)	(0º)					OS: 16.17
24-week Group						
HA/F/2	24 weeks prism	Esotropic	Yes	Yes	Yes	OD: 19.23
(*M mulatta*)	(11.4º BD OD; 11.4º BI OS)					OS: 18.65
QN/F/2	24 weeks prism	Esotropic	Yes	Yes	Yes	OD: 23.28
(*M mulatta*)	(11.4º BI OD; 11.4º BD OS)					OS: 24.01
EY/M/1.5	24 weeks prism	Esotropic	Yes	Yes	Yes	OD: 8.91
(*M mulatta*)	(11.4º BI OD; 11.4º BD OS)					OS: 7.65

BI , base-in; BD, base down; OU, both eyes; OD, right eye; OS, left eye; OKN, optokinetic nystagmus; DVD, dissociated vertical deviation; SSVEP, spatial sweep visual evoked potential; CPD, cycles per degree.

Recordings were performed under conditions of binocular and monocular viewing. Monocular viewing was achieved by use of liquid-crystal shutter goggles which cycled from transparent to opaque (or the reverse) in 80 microseconds (0.08 msec).35 Voltages proportional to horizontal and vertical eye position were digitized at 500 Hz. Eye velocity signals were obtained by passing the eye position signals through a Finite Impulse Response filter (DC to 90 Hz) and differentiated. Angular resolution of the system was about 0.05º. Experiments were controlled and the data were acquired and analyzed with the aid of a computer and interactive signal processing software (Spike2 for Macintosh, Cambridge Electronic Design, United Kingdom, and Igor Graphics, Wave Metrics, Lake Oswego, Oregon).

VISUAL STIMULI AND TRIAL DESIGN

Eye Alignment

In the months before coil implantation, eye alignment was assessed using 35 mm photographs and video recordings of each monkey (Hirshberg method[36,37]). After implantation of eye coils, alignment was measured under conditions of binocular viewing to document precisely the magnitude of any intermittent or constant heterotropia. The fixation target was displaced from primary position (straight ahead) to the cardinal positions of gaze to assess concomitance of any misalignment. Alignment during periods of binocular viewing was compared with alignment when viewing with either eye covered, to reveal the presence of any heterophoria (horizontal or vertical).

Stable Fixation

Viewing monocularly**,** each monkey was required to fixate the laser spot at straight-ahead gaze or at eccentricities of ± 10º horizontally and vertically (Figure 2). The target was presented in repeated trials. In order to receive a juice reward, the animal had to maintain eye position of the nonoccluded, fixating eye within a 2º fixation window, surrounding the target, for a randomized interval of 2 to 5 sec. The small target size, variability of target location, small fixation window, and random duration of required fixation ensured a high level of visual attention.[29]

Smooth Pursuit

Smooth pursuit was recorded under conditions of monocular viewing using a modification of the "step-ramp" paradigm of Rashbass (Figure 2).[38,39] At the beginning of each trial, the animal fixated on the stationary spot at straight-ahead gaze. When the animal's eye remained within a 2º window continuously for an interval of 2 to 5 sec, the stationary spot disappeared and a second spot appeared, moving rightward or leftward at 30º/sec. The moving spot started either from the point of fixation (zero eccentricity) or from 1 of 8

other initial positions along the horizontal meridian (5º and 10º above, below, to the right and left of zero eccentricity). The "step-ramp" approach allowed presentation of target motion at a precise location on the retina as determined by the relative positions of the stationary and moving spots. When viewing with the left eye, rightward target velocities represented nasally directed motion, and leftward target velocities temporally directed stimulus motion in the visual field. To receive the juice reward, the monkey had to track the stimulus within the 2º window for a duration > 750 msec. The onset, direction (up, down, left, right), and speed of the target were controlled by the computer program, which selected combinations of initial target position and direction in a pseudorandom fashion to preclude prediction.

Optokinetic Nystagmus (OKN)

Large-field OKN was evoked under conditions of monocular viewing, using horizontally moving, 100% contrast, vertically oriented, black and white square-wave stripes (0.1 cycle per degree) back-projected on a tangent screen (Figure 2). The stimulus subtended a visual angle of 90° × 90° horizontally and vertically and moved at a velocity of 30°/sec in 60-second trials. The screen was blanked for a period of 90 seconds between all trials to allow dissipation of any OKN after nystagmus.[40]

Disparity Vergence

Horizontal short-latency disparity vergence eye movements were evoked by a stimulus (Figure 3) displayed on a video monitor (for 200 msec) consisting of dots (~1° diameter) on a white background.[41] The stimulus occupied >50% of the animal's visual field. One dot image was visible to the right eye only and the other dot image to the left eye only, ie, dichoptic viewing, which was produced by the use of liquid crystal shutter goggles. The shutters opened and closed alternately before the 2 eyes in synchrony with the right vs left eye video images at 100 cycles per second. In any given vergence trial, the images were separated horizontally on the monitor to create binocular disparities ± 10º in 0.5º steps, evoking convergence (+ disparities) or divergence (- disparities). Catch trials, in which the 2 images superimposed perfectly (ie, 0° disparity), were interleaved in pseudo random fashion. Animals with manifest strabismus were tested with and without prisms of appropriate power, chosen to nullify their angle of horizontal, and when necessary, vertical heterotropia.

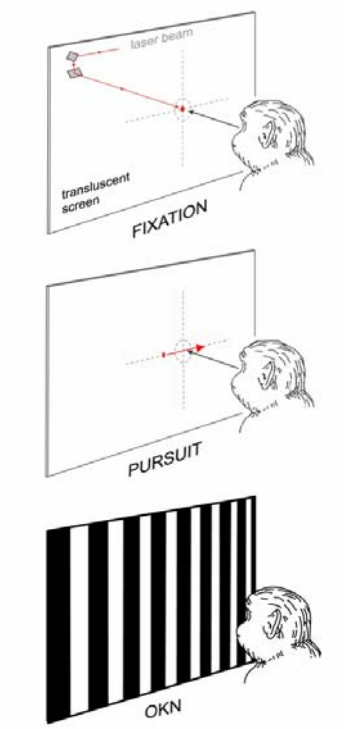

FIGURE 2

Visual stimuli used to test eye alignment and stable fixation, horizontal smooth pursuit, and horizontal optokinetic nystagmus. The moveable stimuli (spot or stripes) were back-projected on a translucent tangent screen.

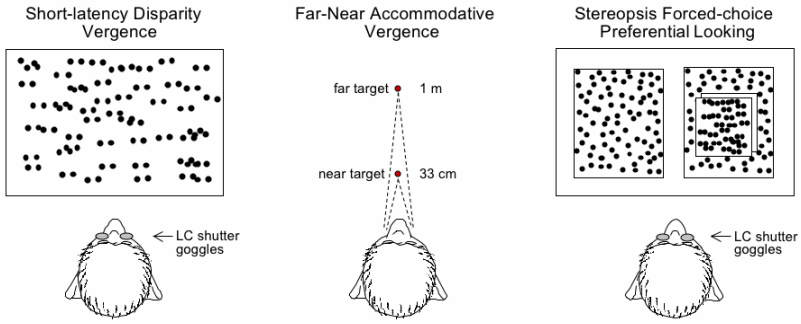

FIGURE 3

Visual stimuli used to test short-latency disparity-vergence, accommodative-disparity vergence, and stereopsis. Monkeys wore liquid-crystal (LC) shutter goggles and viewed correlated-random-dot patterns, displayed on a video monitor, to provide dichoptic viewing in the short-latency vergence and stereopsis trials. Physical far and near LED targets were used to evoke accommodative-disparity vergence.

Accommodative-disparity Vergence

A far target (subtending 0.5º arc) was placed 1 m from the monkey along the midsagittal plane of the head (Figure 3), with a near target (also 0.5º arc) in the same plane 33 cm from the head. The arrangement required the animal to execute a ~3.5º (1.75º each eye) step-change of vergence to the near target and a 2 D step-change of accommodation (from 1 D at the far target to 3 D at near). The angle of vergence demand varied slightly (±0.3º) between monkeys because of differing interocular distances. Combined accommodative-disparity vergence was tested by allowing the monkeys to view with both eyes.[42] Accommodative vergence was tested by occlusion of one eye, eliminating all disparity cues. To initiate a trial the animal had to maintain eye position of the right or left eye within ± 1.5º of the distant target for a randomized interval of 2 to 5 sec, after which the distant target was extinguished and the near target illuminated for an interval of 2 sec. To receive a squirt of juice, the monkey had to respond within 1 second of onset of the near target by moving either eye to within a ± 1.5º window of near target position for an interval of ≥ 1 second.

Random-dot Stereopsis

The forced-choice preferential looking (gaze) technique[43,44] was used to assess stereopsis thresholds (Figure 3). Two random-dot images (squares subtending 20º each), composed of black dots (~ 0.20º diameter) on a white background, were displayed on a video monitor. Dichoptic viewing was achieved by liquid crystal shutter goggles, which opened and closed alternately before the 2 eyes in synchrony with the right vs left eye video images at 100 cycles per second. Each trial began by having the animal fixate a red dot at center position on the blank screen (± 2º) for a random interval of 1 to 5 sec. The center dot then disappeared as the 2 random dot images appeared side by side, separated by a span of 15º. One of the pair of images contained dots that appeared in stereoscopic depth (disparities ranged ± 10º in 0.1º steps). The animal was rewarded for shifting gaze to, and maintaining gaze on, the binocularly disparate image for 3 sec. The position of the disparate image was randomized, left or right, in blocks of 100 trials. Catch trials, in which both images had 0º disparity, were interleaved in pseudorandom fashion. If after repeated testing an animal's correct performance was no better than chance at even the largest disparities, an alteration was introduced: 5 sec after the images appeared, the red dot reappeared at the center of the correct stimulus. This allowed stereo-deficient animals to achieve a reward by eventually executing a correct gaze shift, but discouraged a waiting strategy in stereo-sensitive animals by delaying the reward (monkeys are notoriously impatient). Animals with manifest strabismus were tested with and without prisms that nullified their angle of heterotropia.

Motion VEPs

Motion VEPs were measured using the NUDIVA VEP program developed by Norcia and collegues.[45,46] Three-channel evoked potential recordings were obtained using a bipolar electrode configuration with the active (needle) electrodes 1 cm above the occipital ridge and 2 cm lateral to the sagittal midline, a postauricular reference electrode overlying the region of the mastoid, and a ground electrode near the brow. From a viewing distance of 50 cm, vertical sine-wave gratings (1 to 3 cycles per degree) were displayed using a high-resolution video monitor with a mean luminance of 76.4 candela and a contrast of 84% to stimulate the central 20º of the visual field. The oscillating gratings had the effect of presenting both leftward and rightward motion, each separated in the frequency domain by a 180º phase difference from the other. The animals were tested with 1 cycle per degree gratings presented at 6 Hz, and with 3 cycles per degree gratings presented at 11 Hz. Blocks of 20, 10-second trials per eye were recorded.

DATA ANALYSIS

Eye Alignment

Binocular eye alignment was determined from eye position records, with orthotropia defined as the visual axes of each eye aligned on the fixation spot to within 0.1º of target position during > 90% of rewarded trials. Monkeys who displayed a heterotropia alternated fixation, but typically showed a slight preference for fixation with one eye. The preferred eye was designated as the eye aligned on the target during > 50% of rewarded trials. The heterotropic deviations listed in Table 1 represent the mean eye position of the nonpreferred eye measured from at least 50 fixation trials.

Stable Fixation

Fixation was determined to be stable, ie, fixation nystagmus was absent, if eye position tracings showed no evidence of consistent smooth eye drift when the monkey was rewarded for fixating the stationary spot in primary position or at cardinal gaze positions. Latent fixation nystagmus was assessed as present if a nasally directed slow-phase drift > 0.10º/sec was detected in the tracings of the fixating eye during rewarded trials, accompanied by temporally directed microsaccades (fast phases), which repositioned the target on the fovea. The wave form of nystagmus was characterized by linear or decreasing velocity slow phases, which were superficially conjugate in the fixating and nonfixating eye. Average eye velocity was measured from a minimum of 50 eye position epochs ≥ 500 msec in each animal.

Smooth Pursuit

Individual "step-ramp" trials were judged acceptable for analysis if the trial contained at least 50 msec of smooth eye velocity after the onset of pursuit. If an accepted trial contained a saccade, the saccade was removed and replaced with a straight line using a cursor-controlled interactive computer program. In the case that the linear interpolation did not fit smoothly into the velocity trace, the trial was excluded from analysis. Eye velocity was measured during steady-state pursuit, 150 msec after pursuit onset, from a minimum of 50 identical trials. Nasalward pursuit mean eye velocity (MEV) for the right eye (ie, target motion to the left) and the left eye (ie,

target motion to the right) were pooled, as were temporalward MEVs. A pursuit nasal bias index (NBI) was calculated as: [(nasalward MEV – temporalward MEV)/ (nasalward MEV + temporalward MEV)] × 100.

OKN

The beginning and the end points of a slow-phase trace were marked using a cursor to calculate average velocity for each slow phase. A minimum of 20 slow-phase velocities (SPVs) were averaged within a 60-second trial to obtain mean velocities for nasalward vs temporalward stripe motion, pooling the responses of the right and left eye. An OKN NBI was also calculated.

Disparity Vergence

Vergence angle was defined as the difference between horizontal left eye position and right eye position (LE - RE), with eye positions to the right designated as positive values and to the left negative values. Thus, convergence yielded positive values of vergence and divergence negative values. Unequal movements of the eyes were considered vergence and equal movements were classified as saccades. Vergence velocity and amplitude profiles were compiled by averaging a minimum of 20 responses to each trial disparity.

Accommodative-disparity and Accommodative Vergence

For calculating latencies and amplitudes, onset of eye movement was defined as eye velocity exceeding 10º/sec and initial amplitude was eye position 250 msec after the onset of movement. Trials chosen for analysis were those in which the monkey fulfilled the criteria for stable fixation of the distant target and initiated a convergence or saccadic movement within 500 msec of the target step to the near position. To test accommodative vergence, all disparity cues were eliminated by covering one eye. Mean latencies and amplitudes were calculated from a minimum of 20 far-near target steps.

Random-dot Stereopsis

The presence of stereopsis was measured as gaze directed consistently at the stimulus containing binocularly disparate random dots in repeated trials.[47,48] Eye position was monitored using binocular magnetic search coils. For animals with strabismus, the gaze response was measured as the position of the eye closest to the disparity-containing window at the end of each trial. Several hundred trials were presented in a typical testing session and thresholds established using the staircase method of limits.[49]

Motion VEPs

Data was Fourier transformed to extract the amplitude and phase of the motion VEP at 6 or 12 and 11 or 22 Hz. These peaks of activity represent the first (F1) and second (F2) harmonics of the stimulus presented at 6 or 11 Hz frequency, respectively. The presence of a significant F1 and/or F2 component in the response was determined using the t circ statistic.[46,50] A VEP in which the response to the 2 directions of motion is equal yields a response spectrum that is composed of even multiples of the stimulus frequency (larger F2). An asymmetric VEP contains additional response components at the odd harmonic multiples of the stimulation frequency (larger F1). The symmetry of the motion VEP response was quantified by comparing the relative proportion of F1 to F2. This proportion, called the asymmetry index, was calculated by dividing the amplitude of F1 by the sum of the amplitudes of F1 and F2.[45,51] The asymmetry index can range from 1.0 (extremely asymmetric response dominated by F1) to 0.0 (extremely symmetric response dominated by F2). On the basis of testing a large number of normal human and nonhuman primates, an index greater than 0.25 at 6 Hz, and 0.40 at 11 Hz indicate a directional asymmetry.[51-54]

Overview of Anatomic Methods

A double-labeling technique was used to reveal binocular connections (Figure 4). To identify which ocular dominance columns (ODCs) in layer 4C of V1 were driven by the right vs left eye, one eye in each animal was injected with a radioisotope tracer ([^{3}H] proline).[55,56] The tracer was actively transported in an anterograde manner, trans-synaptically from eye to brain, labeling the V1 territory occupied by ODCs driven by the injected eye (ie the proline was incorporated into retinal ganglion cells within the injected eye and transported by axoplasmic flow to the lateral geniculate body, where it crossed the synapse and was transported via the optic radiations to the striate cortex). ODCs of the fellow, noninjected eye in each hemisphere could be identified as unlabelled V1 territory. To label horizontal, neuronal (axonal) connections between right and left eye ODCs, a second tracer, biotinylated-dextran-amine (BDA), was injected directly into V1 ODCs through burr holes in the skull.[57] The tracer was taken up by axonal terminals within the injected ODC and traveled in a retrograde direction to label connecting, neuronal cell bodies in neighboring ODCs. Active transport of both tracers occurred over a survival time of 1 week. The animals were then perfused with fixative and the occipital lobes removed for histological processing and analysis. These neuroanatomic methods have been described in detail in previous reports[57,58] and for this reason only an abbreviated account is provided here.

Intraocular Tracer Injection

ODCs were labeled using the transneuronal autoradiography protocols of Wiesel and Hubel,[59] and Horton.[60] The monkey was sedated and a 27-gauge needle on a Hamilton syringe was introduced through the pars plana into the midvitreous cavity to inject the [^{3}H] proline solution. The needle was withdrawn from the self-sealing scleral wound and the fundus was examined with an indirect ophthalmoscope to verify absence of retinal trauma.

V1 Ocular Dominance Column Injection

Using standard aseptic technique and general anesthesia, the scalp was incised in the midsagittal plane and on each side, ~ 7 burr holes (3-mm diameter) were drilled in the skull overlying the operculum of the right and left V1. The holes were arranged in a gridlike pattern spaced ~ 0.75 cm apart, extending anterior to the occipital ridge and bordering the midsagittal suture medially. Using a

micromanipulator, glass micropipettes (tip diameter 15 µm) filled with 10% BDA were lowered into the cortex through small slits in the dura to a depth of 0.6 mm. Small volumes (~30 nL) of BDA were injected by applying brief pulses of pressurized air to the back of the pipette. The pipettes were withdrawn and the scalp was sutured closed.

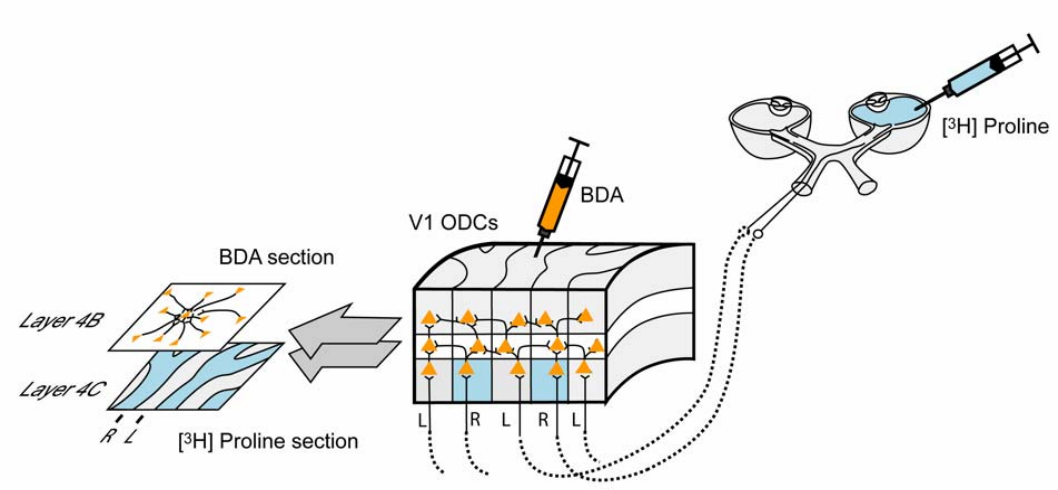

FIGURE 4

Labeling of ocular dominance columns (ODCs) and horizontal axonal connections in striate cortex (area V1) of a normal primate. [^{3}H] proline was injected into the vitreous cavity of one eye and transported anterogradely from eye-to-V1 layer 4C, labeling ODC territory belonging to the injected eye. Unlabeled ODC territory (every-other row of ODCs) belonged to the fellow, noninjected eye. A second label, biotinylated-dextran-amine (BDA), was injected into individual ODCs; it was transported by axonal, horizontal projections, from the site of injection, to label pyramidal neurons in neighboring ODCs, which connected to the injected ODC. Thin, tangential sections through (binocular) layer 4B and (monocular) layer 4C were aligned and overlayed for analysis of horizontal connections.

Euthanasia, Brain Perfusion, and Tissue Processing

The animals were anesthetized deeply and a lethal dose of pentobarbital was administered, followed by perfusion of fixative through the left ventricle using an electric pump. The cerebral hemispheres and brainstem were then removed from the cranium and immersed in a separate container of fixative. The visual cortex was unfolded and flattened, then cut into 40-µm sections on a freezing microtome in a plane parallel to the pial surface. Lateral geniculate nuclei were cut in transverse/coronal sections. To reveal ODCs labeled with [^{3}H] proline, sections were mounted on gelatinized slides, dried, and dipped into a photographic emulsion. The autoradiographs were exposed for 10 weeks, developed, and digitally photographed. To reveal cytochrome-oxidase (CO) patches (blobs) within ODCs, alternate sections of V1 were processed using CO histochemistry.[61]

Analysis of ODCs and Neuronal Connections

To determine the location of the BDA injection sites relative to right-eye vs left-eye ODCs, BDA sections were aligned with [^{3}H] proline sections, using blood vessels as reference marks (Figure 4). The relationships were established and documented by superimposing digital images of BDA- and CO-stained sections, acquired using a Magnafire CCD camera (Optronics, Goleta, California) and software from Soft Imaging System (Münster, Germany). The alignment served as a matrix for the analysis of BDA-labeled patches (composed of terminal axons) as well as labeled pyramidal neuron cell bodies (somata). For individual injections, counts of labeled somata in right-eye ODCs vs left-eye ODCs were obtained in control vs strabismic monkey sections over a distance of 5 to 7 ODCs (a span of 2.5 to 3.5 mm) from the center of the injection. These counts were made from successive, focal planes throughout the thickness of the section. To avoid double counting, the stereological analysis only included somata that were not contained in the preceding focal plane.[62]

The counting method is laborious (~ 100 microscope man-hours/injection site). It was necessary for establishing a strict relationship between labeling patterns viewed at low power, and soma counts at higher power, in representative injections. The volume of injections that needed to be assessed in both hemispheres in each monkey precluded analysis using this technique in all of the monkeys. For this reason, an alternative method was employed. Soma counting revealed a systematic relationship between the overall pattern of labeling, viewed at low power in individual sections, and the soma counts. When the pattern appeared as a "sunburst" distribution of label across ODCs (ie, an oval, densest at the injection center and diminishing uniformly in intensity of

labeling with increasing distance from the center), soma counts showed comparable numbers of labeled somata in right vs left eye ODCs. The diminished intensity of labeling, with increasing distance from the injection center, represents diminishing numbers of connections. Because the "sunburst" pattern showed uniform diminishment across both right and left eye ODC territory, the "sunburst" pattern of labeling was designated the "binocular connection" pattern. Alternatively, when the pattern appeared as a "skipping" distribution of label across ODCs (also densest at the center but fluctuating in intensity of labeling across every other row of ODCs), soma counts showed significantly higher numbers of labeled somata in ODCs, which had the same ocularity as the injected ODC, and significantly lower numbers of labeled somata in the ODCs of opposite ocularity. The "skipping" pattern of labeling was therefore designated the "monocular connection" pattern.

The BDA injections in each V1 hemisphere of each monkey were scored as "sunburst/ binocular" or "skipping/monocular" by 2 observers masked to the animal's behavioral status. Approximately 15% of the injections had ambiguous patterns that could not be scored as either "sunburst" or "skipping" and were excluded. The results of the labeling-pattern scoring are tabulated as bar graphs for each monkey group.

Statistical Methods

An advantage of using primates and operant-conditioning trials is the large number of measurements obtainable for each behavior in each animal. To exploit the size of trial blocks, a nested (hierarchical) analysis-of-variance (one-way ANOVA) was used.[63] Within and between group differences were assessed for each continuous, dependent variable, eg, angle-of-misalignment; nystagmus velocity. Numbers of labeled neuron bodies in adjacent ODCs were compared using a *t* test (one way) for paired samples. The neuroanatomic analysis included measurement of a dichotomous, categorical dependent-variable; between-group differences for these data were assessed using a proportions test.[64] Significance was defined as $P < .05$. To facilitate comparison of the multiple dependent variables, regression lines were plotted (see Figure 27) on the same scale, with the magnitude of the deficit in multiples of standard deviation (for the behavioural data), normalized to the average value of the 3-week monkey group. For the neuroanatomic measure, the regression line plots magnitude as a multiple of the proportion difference ($p = 1 – q$) in the 3-week monkey group.

RESULTS

The results of behavioral testing are described first, and the results of neuroanatomic analysis second. The behavioral results proceed from eye alignment to testing for the constellation of signs that typify the infantile esotropia syndrome in humans. The results in each section compare behaviors by the duration of binocular-decorrelation imposed: control, 3 weeks duration, 12 weeks duration, and 24 weeks duration (hereinafter designated 3-wk, 12-wk, and 24-wk).

EYE ALIGNMENT, CONCOMITANT ESOTROPIA, AND DVD

The control monkeys and the monkeys exposed to 3 weeks of binocular decorrelation had normal horizontal and vertical eye alignment when tested at age 1 year. In contrast, the 12-wk and the 24-wk monkeys exhibited constant esotropic strabismus. The 24-wk monkeys (Figure 5) had the largest angles. Plots of eye alignment for individual monkeys during cover-testing at cardinal gaze positions are shown in Figure 6. Automated alternate-cover testing revealed small (< 1.7º) heterophorias in control monkey AY and 3-wk monkey SY; they exhibited no misalignment when viewing binocularly (not shown). The single-cover test results of Figure 6 show that monkey GO (12-wk) had an esodeviation of 7.1 ± 1.4º, and monkey HA (24-wk) an esodeviation of 13.2º ± 2.1. The deviation in each of these animals was constant when they viewed with both eyes uncovered, confirming that these were not merely esophoric misalignments. The esotropic deviations were concomitant, and no striking A or V patterns were evident.

The 12-wk and each of the 24-wk monkeys also showed DVDs,[65,66] ranging in magnitude from 2.0 to 7.1º. The 12-wk monkey GO manifested, in addition to the DVD, a dissociated horizontal deviation when fixating with the left eye (right-eye dissociated horizontal deviation (DHD), Figure 6).[67,68] As in human esotropes, the DVDs differed in magnitude in the 2 eyes. Figure 6 shows a larger DVD in monkey GO (12-wk) when fixating with the right eye, and a larger DVD in monkey HA (24-wk) when fixating with the left eye. Only the DHD of the right eye in monkey GO conformed to a V pattern; the esotropia measured with both eyes uncovered showed no noteworthy pattern.

Concomitancy of the horizontal and vertical deviations across 5 cardinal gaze positions is shown for each of the duration groups in the bar graphs of Figure 7. The magnitude of the heterophorias is plotted in the control and 3-wk monkeys, and the magnitude of the heterotropias in the 12-wk and in the 24-wk monkeys. Magnitudes were substantially greater in the 12- and 24-wk animals (ANOVA, $P = .008$).

To appreciate the significance of these findings, it is important to emphasize a methodological point: the direction of the horizontal strabismus cannot be explained as adaptation of the fusional vergence system to optical prisms (prism adaptation).[69,70] As illustrated in Figure 8, the horizontal prism was positioned base-in, displacing the image off the fovea and onto the eccentric nasal hemiretina in each experimental animal. If the animals had attempted to overcome the horizontal component of the decorrelation by prism adaptation, they would have diverged their eyes into an exotropic position. But each of the monkeys (Table 1 and Figure 5) developed convergent strabismus. The finding of DVDs in the strabismic animals can, likewise, not be explained as vertical prism adaptation. Cover-testing did not show a hypertropia in one eye and a hypotropia in the other; both eyes had hyperdeviations (Figure 6), which is the hallmark of DVD.

As noted in the "Methods" section, the infant monkeys manifested esotropic deviations after wearing the prisms for a period of ~ 1 to 2 weeks (observed by infrared viewing during daily goggle cleaning and estimated by Hirschberg measurement to be, on average ~

8 º to 10º). A physical esotropia of ~ 10º added to a base-in prism displacement of 11º sums to a total magnitude of horizontal-image noncorrespondence of ~ 21º. Removing the goggles after 3 to 24 weeks of prism-rearing achieved, therefore, a reduction in binocular noncorrespondence of ~ 50%. Extrapolating to an esotropic human infant, this was the sensorial equivalent of correcting the esotropia by 50% (ie, surgical undercorrection). The results of Figures 5 through 7 show that a 50% correction was effective for recovery of normal alignment if carried out by age 3 weeks, but was ineffective if delayed to age 12 to 24 weeks. Unfortunately, the time-course for the recovery of eye alignment after goggle removal in the 3-wk monkeys (hours, days, or weeks) is not known. By age ~ 4 months, when they were shipped from the nursery in Atlanta to the author's lab in St Louis, eye alignment by Hirschberg measurement was orthotropic.

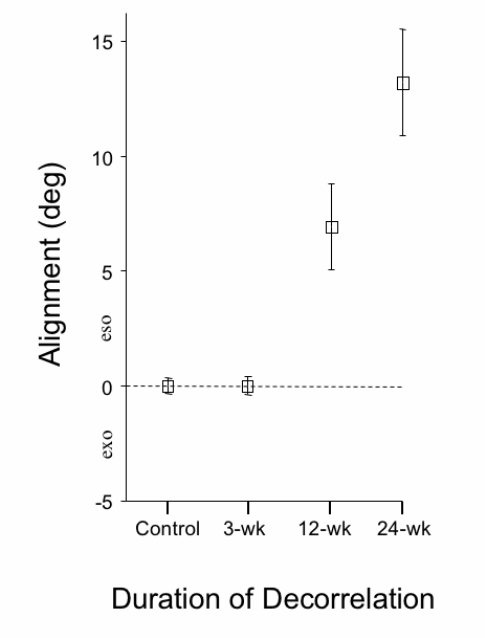

FIGURE 5

Eye alignment at age 1 year measured under conditions of binocular (neither eye covered) viewing. Group means ± SD for straight-ahead (primary position) gaze.

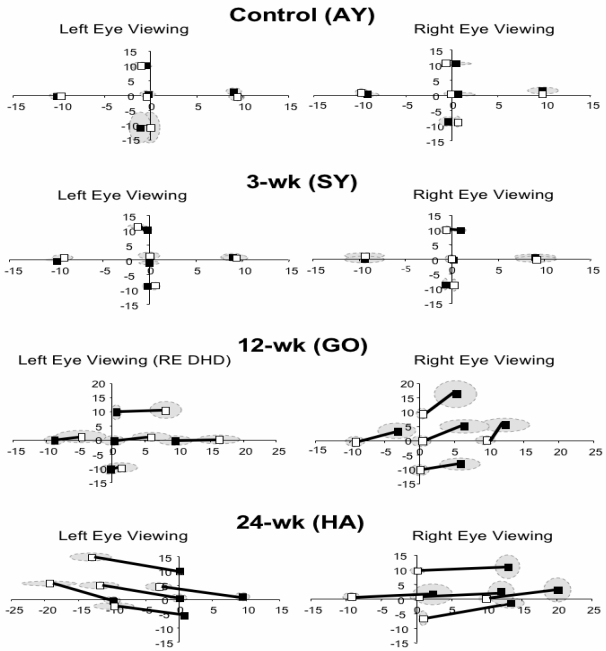

FIGURE 6

Eye alignment at age 1 year measured during automated, single-cover testing at 5 cardinal gaze positions. Control monkey AY and 3-wk monkey SY had small heterophorias. 12-wk monkey GO was esotropic, shown here when fixating with the right eye. This animal often displayed a right-eye dissociated horizontal deviation (DHD) as shown when fixating with the left eye. The dissociated vertical deviation (DVD) in the right eye is smaller than that in the left eye. 24-wk monkey HA had both a larger esotropia and larger DVDs. Mean ± SD (range indicated by shading).

VISUAL ACUITY AND ABSENCE OF AMBLYOPIA

As shown by the visual acuities listed in Table 1, none of the strabismic monkeys had strabismic amblyopia (defined as an interocular acuity difference ≥ 0.25 octave).[71,72] Grating visual acuity thresholds, as measured by SS VEP (Table 1), varied idiosyncratically from animal to animal, but interocular acuity differences were comparable in experimental and control monkeys. Acuities were not related systematically to refractive error (SSVEPs were recorded without refractive correction; refractive errors were ≤ + 3.00 spherical equivalent in each of the experimental and control animals). Fresnel prisms were used in the experimental monkeys and plano lenses in the controls. In addition to image decorrelation, Fresnel prisms can cause some image blur and mild chromatic aberration.[73] The Fresnel prisms did not impair development of acuity; both the lowest and highest acuities recorded were in the 24-wk strabismic monkey group. These acuity ranges, and small interocular acuity differences, are similar to those of normal, adult macaques measured in the author's laboratory. The strabismic monkeys would alternate fixation, but like most humans with alternating esotropia, often displayed a preference for fixation with one eye.

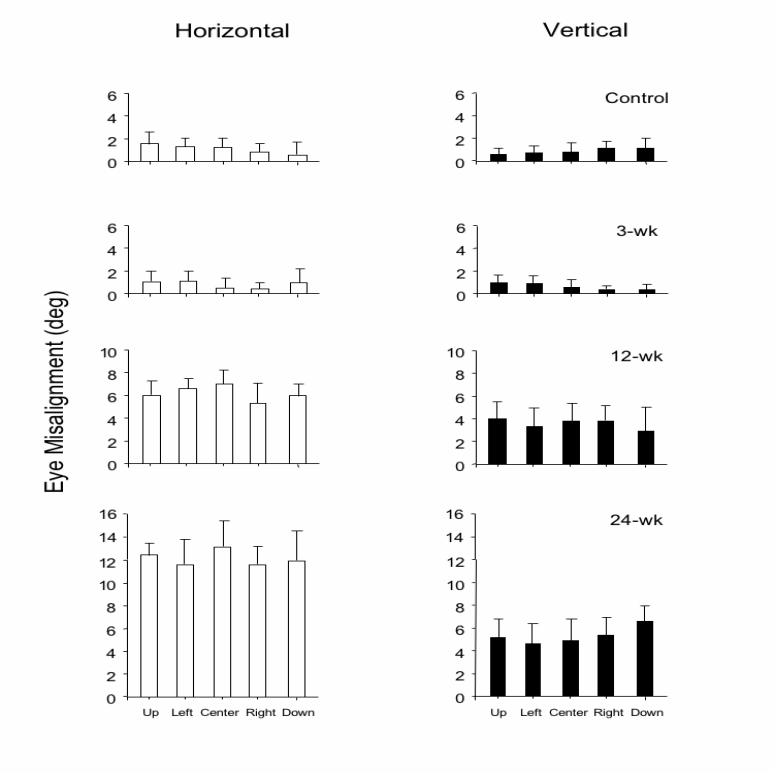

FIGURE 7

Horizontal and vertical eye misalignment measured during single-cover testing at 5 gaze positions in the 4 groups of monkeys. Group means ± SD.

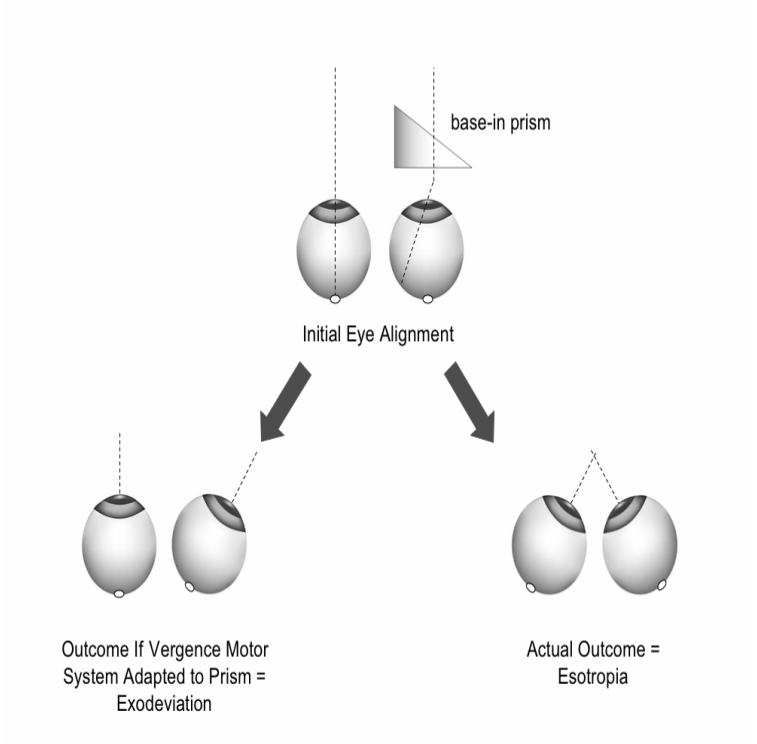

FIGURE 8

Absence of prism-adaptation, and deterioration to esotropia caused by noncorresponding binocular images.

LATENT FIXATION NYSTAGMUS

The control and 3-wk monkeys had stable fixation when viewing monocularly or binocularly (Figure 9A and 9B). The 12-wk monkey and the 24-wk monkeys, however, showed latent fixation (fusion maldevelopment[74]) nystagmus, more pronounced in the 24-wk animals. The nystagmus was evident as nasalward slow-phase drifts, with respect to the fixating eye, interrupted by temporalward fast phase jerks (Figure 9C and 9D). The wave-form of the slow-phase—decreasing or linear velocity—conformed to standard latent nystagmus criteria.[40] The nystagmus was conjugate to casual "clinical" inspection: the direction and frequency were the same in both eyes. Analysis of eye position tracings revealed consistent disconjugacy of velocity and amplitude, with oscillations damped in the fixating-eye and accentuated in the deviated eye. The records of Figure 9C and 9D also show that the nystagmus persisted, but was less pronounced, when viewing with both eyes uncovered, ie, manifest-latent nystagmus.

Average slow-phase velocities of the latent and manifest-latent nystagmus are shown in Figure 10. The largest mean velocity, 2.0º/sec was recorded during monocular viewing in the 24-wk monkeys (ANOVA, $P = .02$). Nystagmus velocity during binocular viewing was 26% to 51% slower. Nystagmus intensity (the product of frequency × amplitude) increased systematically with increasing duration of decorrelation (Figure 11; ANOVA, $P = .001$).

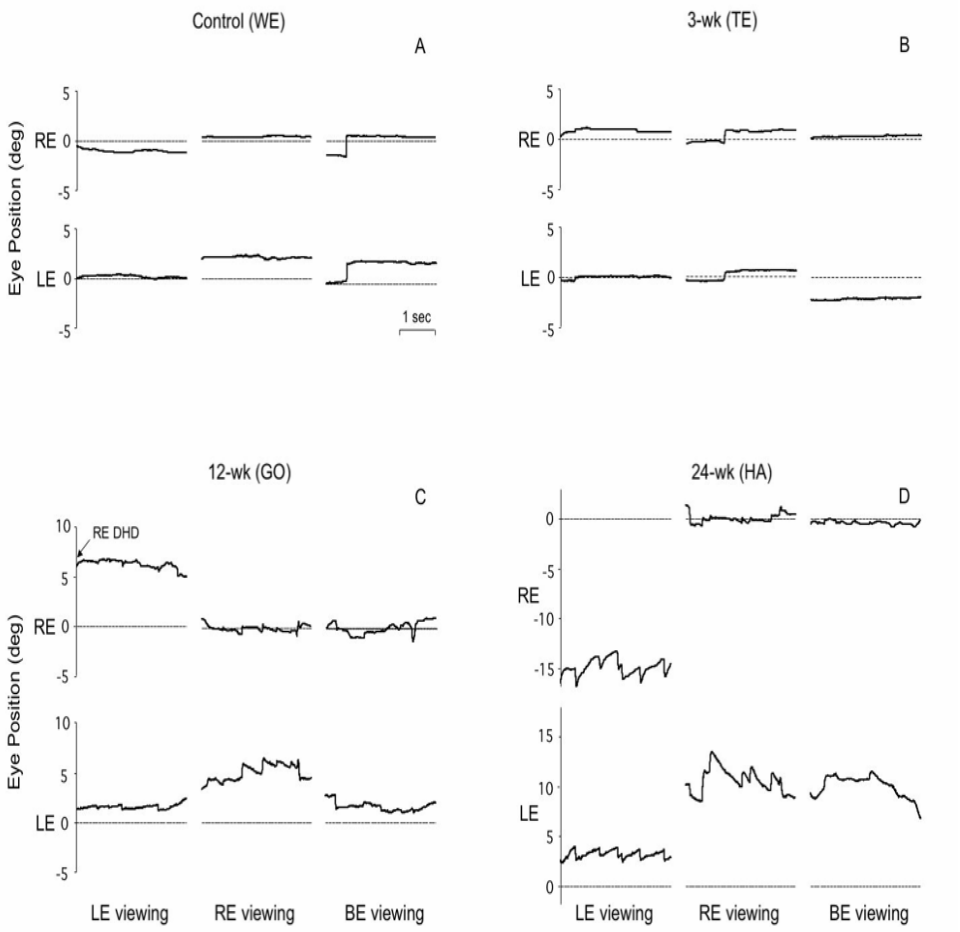

FIGURE 9

Stable fixation vs latent/manifest latent nystagmus in horizontal eye position tracings from 4 monkeys; fixating monocularly with the right eye (RE) or left eye (LE) covered, and viewing binocularly. A and B, Stable fixation in control monkey WE and 3-wk monkey TE. C, Latent nystagmus, manifest-latent nystagmus and right-eye dissociated horizontal deviation (DHD) in 12-wk monkey GO. D, Latent and manifest-latent nystagmus in 24-wk monkey HA. Nystagmus tended to be lower velocity in the fixating eye. Upward = rightward eye position.

NASOTEMPORAL ASYMMETRIES OF PURSUIT

Figures 2 and 12 illustrate the "step-ramp" strategy used to present image motion and elicit pursuit. The trials of Figure 12A were obtained from control animal (AY) viewing with the right eye. The stationary fixation spot (at 0º straight ahead) disappeared after an

unpredictable duration. Simultaneously, the tracking target appeared at 5º to the left (for temporalward tracking) or right (for nasalward tracking) and started to move in the opposite direction at 30º/sec (Figure 12A, upper panel). With a latency of ~ 80 msec, the eye accelerated from zero velocity and achieved the velocity of the target (steady state) after approximately 150 msec of pursuit (Figure 12A, lower panel). Note that pursuit eye velocity was equally strong for both temporalward and nasalward target motion (velocity response envelopes are plotted for each direction, with a mean eye velocity line bracketed by ± 1 SD velocity lines).

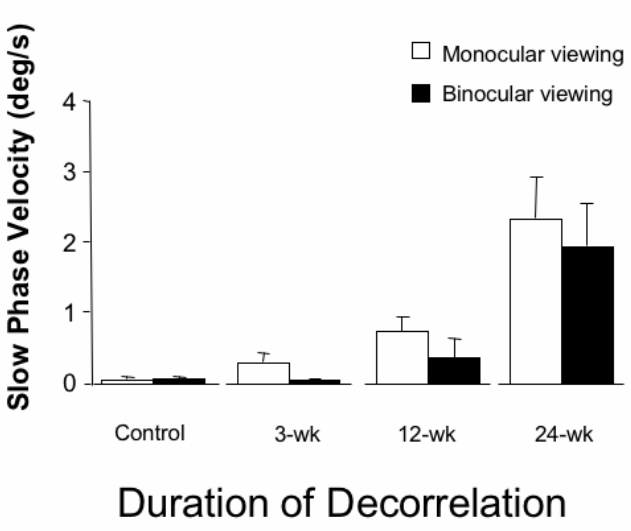

FIGURE 10

Velocity of latent and manifest-latent nystagmus in the 4 groups of monkeys. Group means ± SD; pooled responses of right and left eye.

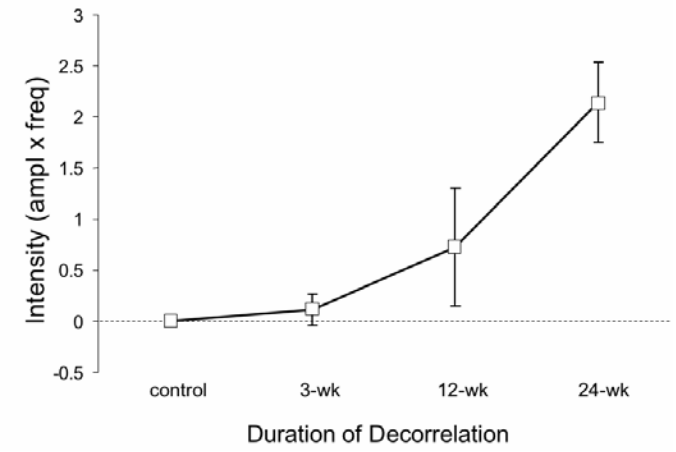

FIGURE 11

Intensity of latent and manifest-latent nystagmus in the 4 groups of monkeys. Group means ± SD; pooled responses of right and left eye.

The 3-wk monkey shown in Figure 12B also demonstrated symmetrical pursuit for both temporalward and nasalward stimulus motion. In contrast, in the 12-wk (Figure 12C) and 24-wk (Figure 12D) animals, a nasotemporal asymmetry of pursuit was evident. Their responses also tended to be more variable and less machinelike. Pursuit for temporalward stimulus motion was less robust, evident as eye position lagging target position (upper panels) and eye velocity (lower panels) that was, on average, 16% to 49% lower than that for nasalward motion. Pursuit latencies did not differ between monkey groups (ANOVA, $P = .24$)

Nasotemporal pursuit performance was compared for target velocities of 15º/sec and 30º/sec, across monkey groups, by calculating a nasal bias index (NBI, defined as the difference, divided by the sum, of nasalward and temporalward mean smooth eye velocity; see "Methods" section). An NBI of zero would indicate symmetrical pursuit, a positive NBI stronger nasalward, and a negative NBI stronger temporalward pursuit. The NBIs for the 4 groups of monkeys are shown in the bar graphs of Figure 13. Pursuit was symmetrical in both the control and 3-wk groups, who had NBI ≤ 1. Pursuit was nasally biased in the 12-wk and 24-wk monkeys, with the largest NBI in the 24-wk animals (ANOVA for mean temporalward velocities, $P = .04$).

NASOTEMPORAL ASYMMETRIES OF OKN

Figure 14 shows representative OKN responses viewing with the left eye. In both normal control (Figure 14A) and 3-wk monkeys (Figure 14B), responses were equivalent for both nasally directed and temporally directed large-field (90 × 90º) stimulus motion. However, both the 12-wk (Figure 14C) and the 24-wk (Figure 14D) monkeys exhibited a directional asymmetry. OKN was stronger and more consistent for nasally directed motion. Temporalward motion evoked lower slow-phase velocities and fewer epochs of sustained nystagmus.

Figure 15 plots a NBI for OKN in each of the 4 monkey groups. Symmetrical nasotemporal OKN responses in the control and 3-wk monkeys produced NBI ≤ 2. The NBI in the 12-wk monkey was 10 times higher (= 20.2) and in the 24-wk 18.5 times higher (= 37.1; ANOVA for mean temporalward SPV, $P = .000$). It is important to note that the directional biases of pursuit and OKN cannot be explained, as latent nystagmus drifts, merely adding to a nasalward response and subtracting from a temporalward response. Latent nystagmus slow-phases, averaging ~ 0.75º/sec in the 12-wk monkey, and ~ 2.0º/sec in the 24-wk monkeys, would produce NBI of 2.5 and 6.7, respectively, when factored into a perfectly symmetric response to 30º/sec target motion. The actual NBI for 30º/sec pursuit in these animals was 5.1 (12-wk) and 22.5 (24-wk). For OKN, the actual NBI was 20.2 (12-wk) and 37.1 (24-wk). Thus, the actual NBIs were 104% to 554% higher than could be accounted for by any influence of nasalward-drift nystagmus.

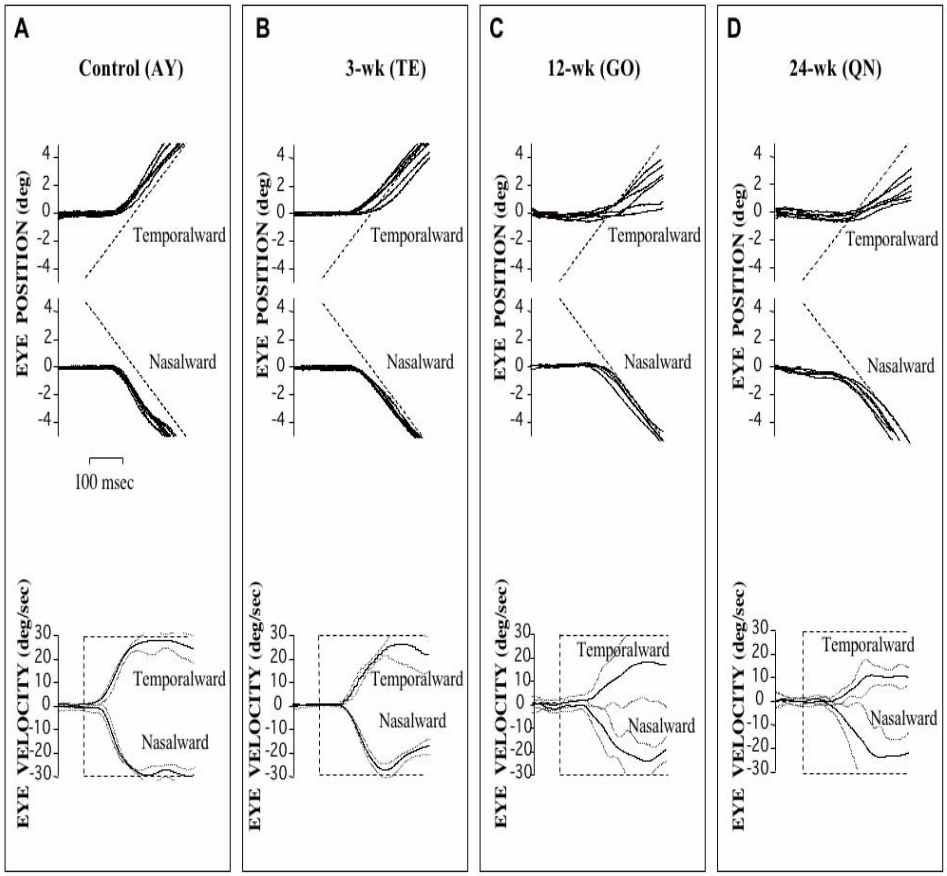

FIGURE 12

Horizontal smooth pursuit for nasalward vs temporalward target motion, viewing with the right eye (left eye occluded). In both the control (A) and 3-wk monkey (B), horizontal pursuit was equally robust for nasalward vs temporalward motion. In contrast, the 12-wk monkey (C) and 24-wk monkey (D) showed a nasotemporal asymmetry, evident as lower-velocity pursuit in response to temporalward motion. Eye position (upper panels) and eye velocity (lower panels); 10 trials for each direction; upward deflections = rightward movements; eye velocity profiles = mean ± SD.

SHORT-LATENCY DISPARITY-VERGENCE RESPONSES

Fusional vergence in normal monkeys and humans has been divided into 2 components, which appear to subserve different binocular functions.[40,75] Short-latency (ie, 50 to 80 msec) vergence is driven by small disparities, typically 2.5º or less. A preceding saccadic eye movement facilitates it, and its chief function may be to correct the small vergence errors that occur at the end of conjugate saccades (normal abducting saccades typically lead adducting saccades, causing physiologic disjunctive errors).[41] Longer-latency (150 to 250 msec) vergence responds to larger disparities (up to ~ 10º) during fixation and is boosted by accommodative (blur) cues. Both components of the vergence response were tested in the 4 groups of monkeys to determine whether they were affected differently.

The stimulus used to evoke short-latency disparity vergence was a large, correlated-dot pattern displayed on a video monitor, viewed through liquid-crystal shutter goggles (Figure 3). By varying the horizontal offset of the dot patterns viewed by the right vs left eye, pure binocular disparity could be produced, devoid of any accommodative, monocular cues. Figure 16 shows short-latency convergence and divergence eye velocity tracings in response to disparities of - 0.5 to + 1.0º, presented at time-0 on the y-axis. Each tracing represents an average of 10 trials at that disparity. The control (WE) and 3-wk monkey (TE) had appropriate convergent (+) and divergent (-) velocity deflections at ~ 60 msec, with the 3-wk animal generating more robust velocities than the control. In contrast, the 12- (GO) and 24-wk (QN) animals displayed erratic vergence-velocity baselines and no convincing disparity responses (ANOVA, velocities at +0.5º, P = .01). The 12- and 24-wk monkeys were also tested in sessions using base-out Fresnel prisms to offset the esotropia and optically re-align the eyes. Performance did not improve.

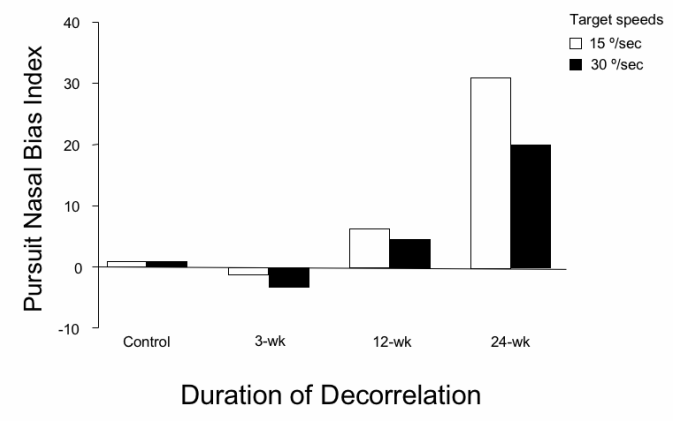

FIGURE 13

Nasalward biases of smooth pursuit as a function of decorrelation duration. Group means ± SD; pooled responses for right and left eye viewing.

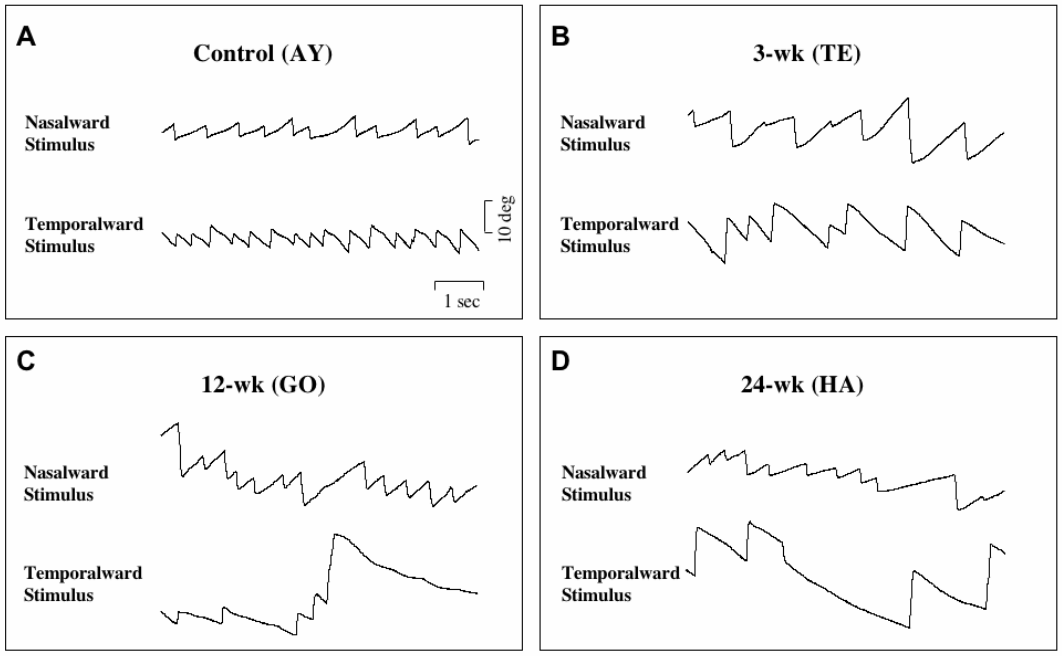

FIGURE 14

Horizontal optokinetic nystagmus for nasalward vs temporalward target motion, viewing with the left eye (right eye occluded). In both the control (A) and 3-wk monkey (B), responses were equally robust for nasalward vs temporalward stripe motion. In contrast, the 12-wk monkey (C) and 24-wk monkey (D) showed a nasotemporal asymmetry, evident as lower slow-phase velocities and fewer fast-phases of nystagmus for temporalward motion. Upward deflections = rightward movements.

Figure 17 shows change in short-latency vergence, for monkeys in each group, over a wider range of disparities. The control (WE) and 3-wk monkey (TE) had the most systematic responses, with the largest amplitude divergence and convergence responses in the 3-wk monkey. The responses of the 12- and 24-wk strabismic animals were unsystematic and at some disparities inverted ("wrong-way"), not coupled to either the magnitude or sign of the stimulus (ANOVA, amplitudes at +1º and +2º, $P = .04$).

ACCOMMODATIVE-DISPARITY VERGENCE, ACCOMMODATIVE VERGENCE AND AC/A

Accommodative-disparity vergence was evoked by physical far and near LED targets. Unlike the correlated-dot stimulus used for short-latency disparity vergence, the LED targets provided both accommodative blur and binocular disparity cues. The step-change in depth of the target in these sessions required the monkeys to change accommodation 2 D and converge 3.5º to achieve accurate bifixation on the near target.

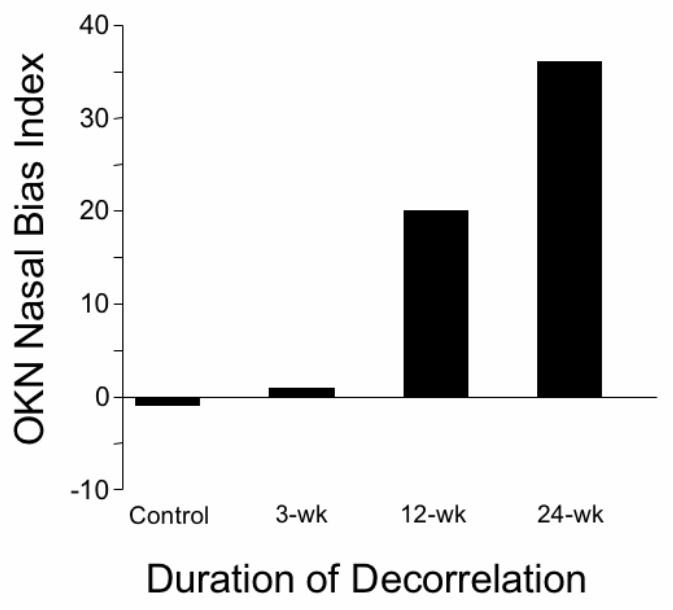

FIGURE 15

Nasalward biases of optokinetic nystagmus (OKN) as a function of decorrelation duration. Group means ± SD; pooled responses for right and left eye viewing.

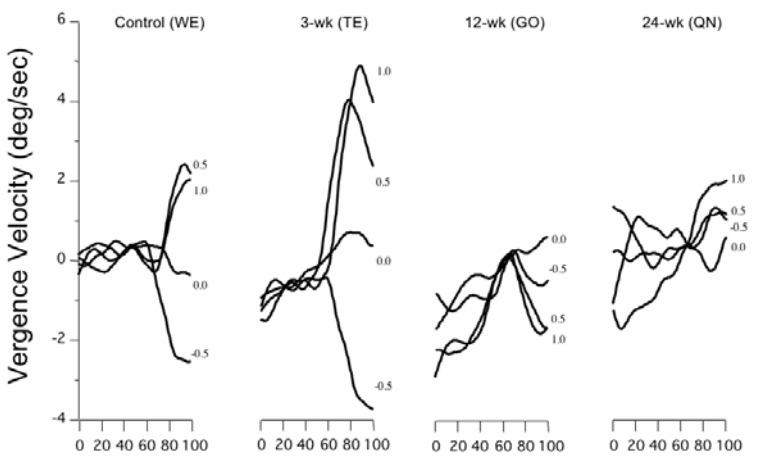

FIGURE 16

Velocity of short-latency fusional vergence in response to binocular disparities of -0.5 to +1.0º. The control and 3-wk monkey had comparable, robust responses. The 12- and 24-wk monkeys had negligible or inverted responses, with noisier velocity baselines. Averages of a minimum of 20 trials at each disparity. Latency of response was ~ 50 to 75 msec after onset of stimulus. Positive values = convergence; negative values = divergence.

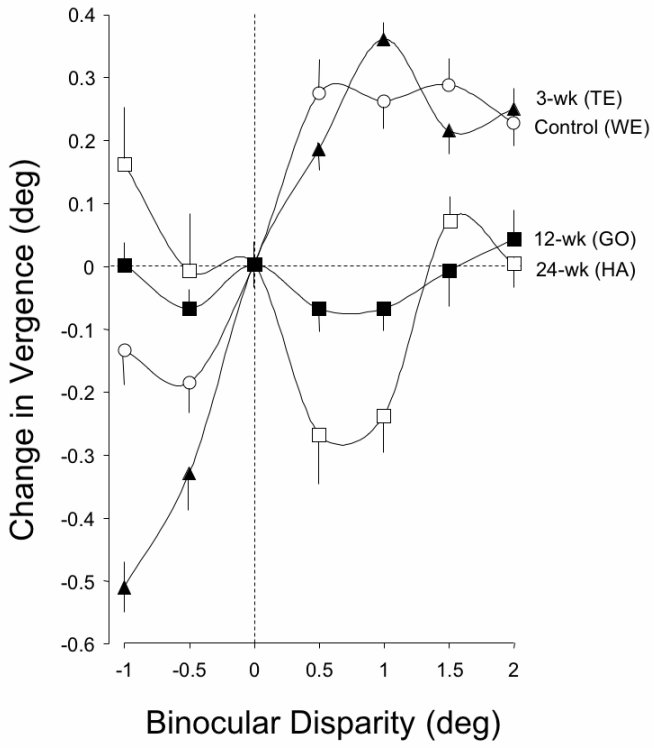

FIGURE 17

Amplitude of short-latency fusional vergence in response to binocular disparities of -1 to +2º. The control and 3-wk monkey had comparable response profiles for disparities of -0.5 to +2º. The 12- and the 24-wk monkeys showed negligible or wrong-way responses across the entire range of disparities. Averages (mean ± SD) from 20 trials at each disparity.

As shown in Figure 18, control monkey AY executed accurate, stereotyped convergence eye movements when the target stepped from far to near. The animal converged an average of 3.35 ± 0.5º, or 96% of the near-target vergence angle. The right eye adducted an average of 1.72º and the left eye an average 1.63º. The average latency of the initial response was 136 ± 11 msec. The 3-wk monkey SY (Figure 18) also executed robust convergence, albeit not as systematically as normal monkey AY. In the 10 trials shown, the near-target was situated minimally to the right of SY's midsagittal plane, which required the left eye to converge (adduct) 0.6º more than the right. (The near-target in these sessions was aligned as accurately as possible on the midsagittal plane ["cyclopean center"] of the head with the goal of requiring perfectly symmetric vergence in the 2 eyes. However, the head restraint device in each animal held the skull firmly but not rigidly, and owing to the powerful neck musculature of macaques, head translational displacements of ~ 1 mm to the right or left of the midsagittal plane were unavoidable.) The convergence response in SY was 3.01 ± 1.1º, or 86% of target vergence, at an average latency of 165 ± 17 msec.

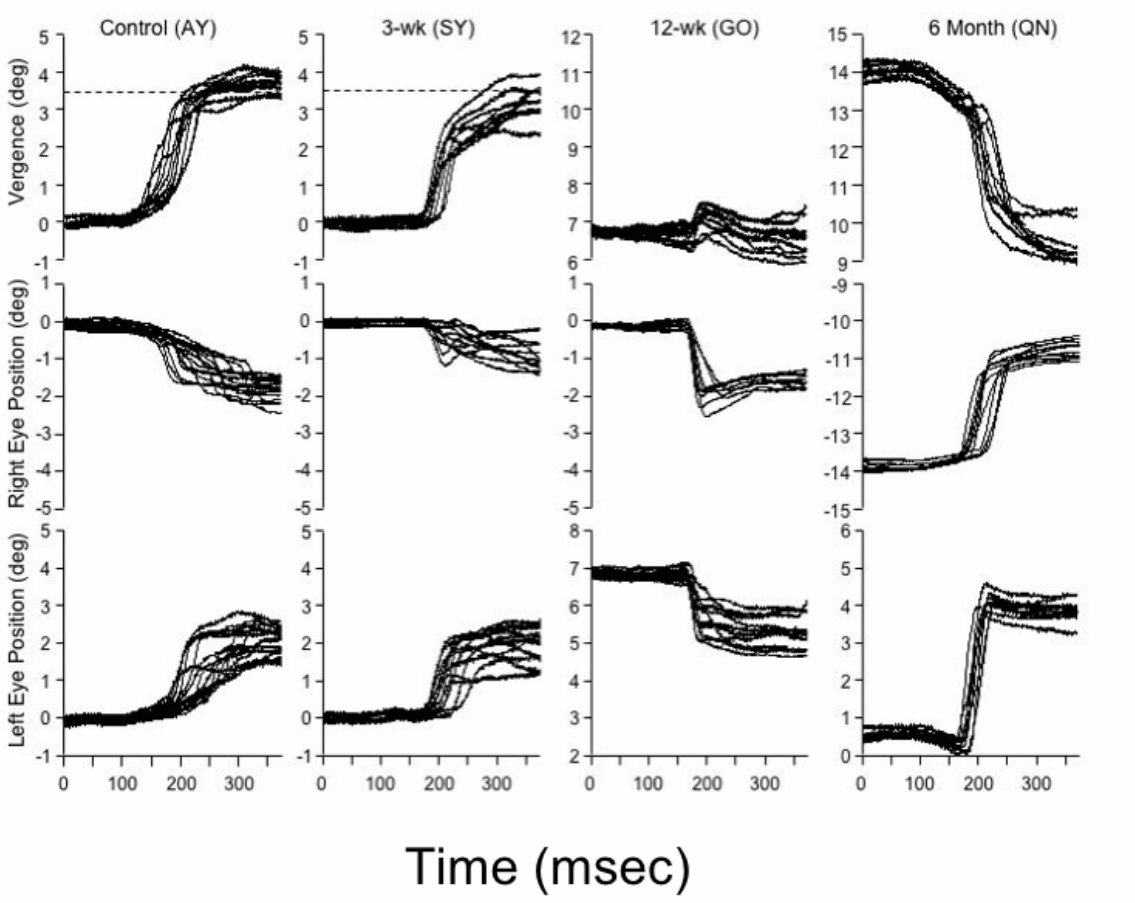

FIGURE 18

Accommodative-disparity vergence in response to a step-change in position of target from far to near (vergence demand ~ 3.5º, or ~ 1.75º/eye). Target jump to near position occurred at "0 msec" on the x-axis. The responses of the control and 3-wk monkey were comparable, with a slightly asymmetric vergence response: greater amplitude of movement in the left eye. The 12-wk esotropic monkey fixated with the right eye. He made disconjugate saccades in each eye, allowing the right eye to refixate the near target; convergence was subnormal. The 24-wk esotropic monkey fixated with the left eye, and made variable, disconjugate, overshooting rightward saccades to refixate the near target.

The accommodative-disparity vergence responses of the esotropic monkeys GO (12-wk; esotropia ~ 7º) and HA (24-wk; esotropia ~ 13º) differed strikingly from that of the control and 3-wk monkey. Rather than smoothly converging, both of the strabismic monkeys (Figure 18) employed a variable, disjunctive-saccade strategy. The saccades in monkey GO adducted the fixating-right eye to the near target. The saccades in monkey HA adducted the fixating-left eye toward the near target, but consistently overshot target position. The saccades were disjunctive: in 12-wk monkey GO they achieved convergence of an average 1.1º, and in 24-wk monkey HA convergence of an average 0.52º. The mean latencies of the saccadic responses (168 ± 18 msec in GO; 175 ± 14 msec in QN) were comparable to the vergence responses of the control and 3-wk monkeys (ANOVA; $P = .07$). Convergence performance, measured as vergence amplitude as a percentage of near target position, is summarized for the 4 monkeys in the bar graph of Figure 19. The

convergence of the strabismic 12- and 24-wk monkeys was deficient compared to the control and 3-wk monkey (n = 50 trials, ANOVA P = .01). The behavior of the 12- and 24-wk esotropic monkeys was similar to that reported in monkeys with natural infantile esotropia.[42] Natural esotropes also execute disjunctive saccades to refixate near targets and have subnormal vergence.[42,76] Saccadic peak velocities were compared in control and experimental monkeys, for saccade amplitudes from 5º to 25º. The esotropic monkeys had peak velocities ("main sequence plots"[40]) that fell within the range recorded in controls, confirming absence of lateral rectus paresis or abducens palsy.

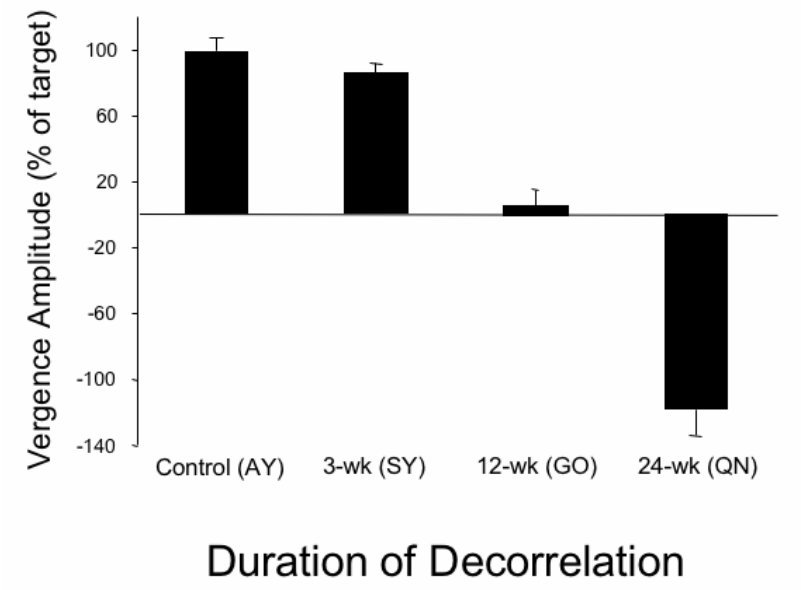

FIGURE 19

Accommodative-disparity convergence amplitude as a percentage of target step to the near position. The control and 3-wk monkey had comparable responses. The 12-wk monkey showed a subnormal response; the 24-wk monkey showed an even weaker response. Mean ± SD.

To test accommodative vergence, binocular disparity cues were eliminated by recording vergence to the near target under conditions of monocular viewing (ie, the paradigm remained the same, but one eye was occluded). In normal adult monkeys, monocular viewing reduces the amplitude of the vergence response by ~ 20%.[42,77] In the control and 3-wk monkeys of the current study, monocular viewing reduced the amplitude of the convergence responses an average of 25% and 19%, respectively (data not shown). The disjunctive-saccade behavior of the 12- and 24-wk monkeys was unaltered, reinforcing the point that their saccades—even with both eyes open—were driven by monocular position and blur cues, rather than sensitivity to binocular disparity.

The synkinetic relationship between accommodative-convergence and accommodation is expressed clinically as a ratio (AC/A, in prism diopters/sphere diopters with 1 prism diopter = 0.57º).[40] A "stimulus AC/A ratio" is measured in the typical clinical setting with the assumption that lens accommodation matches the accommodative demand of the near target to eliminate all blur. Measurement of an actual "response AC/A" requires recording with an optometer.[78] A stimulus AC/A ratio was measured in each of the monkeys with the assumption that they carried out the 2.0 D change of accommodation demanded to focus on the near target (the distant target [1 meter] demanded 1.0 D of accommodation and the near target [0.33 meter] demanded 3.0 D, where D = 1/target distance in meters). The stimulus AC/A ratios in control monkeys averaged 2.31 and in the 3-wk monkeys 2.24. These values agree both with stimulus AC/A ratios and response AC/A ratios (2.0 to 3.0) reported for normal, adult macaques.[77,42] The very weak accommodative vergence response of the 12-wk esotropic monkey GO yielded a low stimulus AC/A ratio: 0.55. The stimulus AC/A in the two 24-wk monkeys was lower, an average of 0.27.

RANDOM-DOT STEREOPSIS

Stereopsis thresholds for random-dot stimuli were measured using a preferential-looking paradigm over a disparity range ± 5º. In each trial, the monkey viewed 2 stimuli presented side by side on a video monitor: one stimulus was flat (zero binocular disparity) and the other contained a patch of crossed (near) or uncrossed (far) disparity. The stimulus display allowed measurement of stereopsis down to ± 0.1º (360 arc sec).

Figure 20A shows the responses of a control monkey (AY). He displayed stereo-sensitivity (ie, a minimum of 70% correct) over the entire range tested, with responses falling to chance level only for interleaved, zero-disparity, "catch" trials. The 3-wk monkey (SY) also showed normal stereo-sensitivity (Figure 20B). In contrast, 24-wk monkey HA proved to be stereo-blind (Figure 20C), as was 24-wk monkey QN (not shown). Optically realigning the eyes of the 24-wk monkeys with Fresnel prism did not improve their performance. (Broken eye movement coils near the end of behavioral testing prevented measurement of stereopsis in 12-wk monkey GO). Figure 21 plots the responses to larger (Figure 21A) and smaller (Figure 21B) disparities. Performance declined for smaller disparities, even in the control animal.

MOTION VEP ASYMMETRIES

Work in human infants has shown that the presence or absence of motion VEP asymmetry is strongly tied to ocular motor fusion.[79,80] Motion VEPs are asymmetric in normal infants before the onset of binocular alignment and fusional eye movements, but symmetric once alignment and fusion are established. In infants with esotropia who were repaired by eye muscle surgery, the prevalence of asymmetric VEPs is significantly lower in those who regain fusion postoperatively. Motion VEPs were recorded during monocular viewing, and asymmetry indices calculated (see "Methods" section), for stimulus spatial-temporal frequencies of 1 cycle per degree/6 Hz and 3 cpd/11 Hz in each animal.[54]

Mean asymmetry indices for each of the 4 groups of monkeys are summarized in the bar graphs of Figure 22. When tested using 1-cpd gratings that oscillated at 6 Hz, mean asymmetry indices were < 0.25 (indicated by the horizontal dashed line) for the control and 3-wk monkeys, but 0.55 ± 0.32 in the 12-wk, and 0.51 ± 0.29 in the 24-wk esotropic animals (ANOVA, $P = .01$). Similar results were obtained when testing was performed using 3-cpd gratings that oscillated at 11 Hz. The mean asymmetry index was < 0.40 (dashed line) in controls (0.38 ± 0.05) and 3-wk (0.31 ± 0.03) monkeys, but measured 0.72 ± 0.18 in the 12-wk and 0.76 ± 0.23 in the 24-wk esotropic monkeys (ANOVA, $P = .008$).

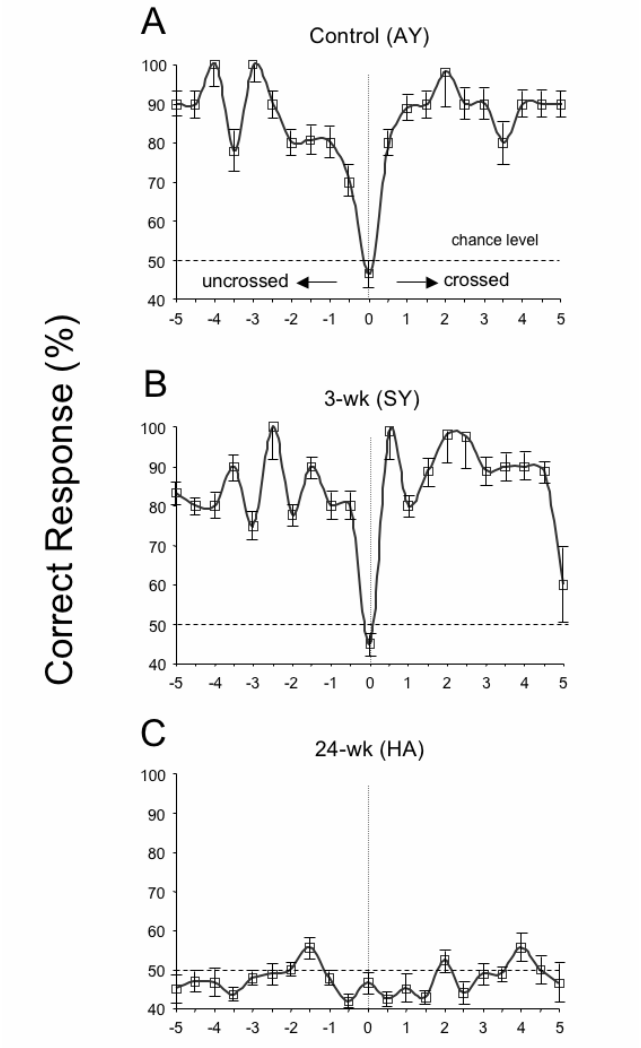

FIGURE 20

Random-dot stereopsis for disparities ± 5º. The control and 3-wk monkey had equivalent levels of stereoscopic sensitivity over the entire range. The 24-wk monkey was stereoblind; esotropic monkey tested with prisms to realign the visual axes. 50% dashed line = chance level of performance**.** Means ± SD.

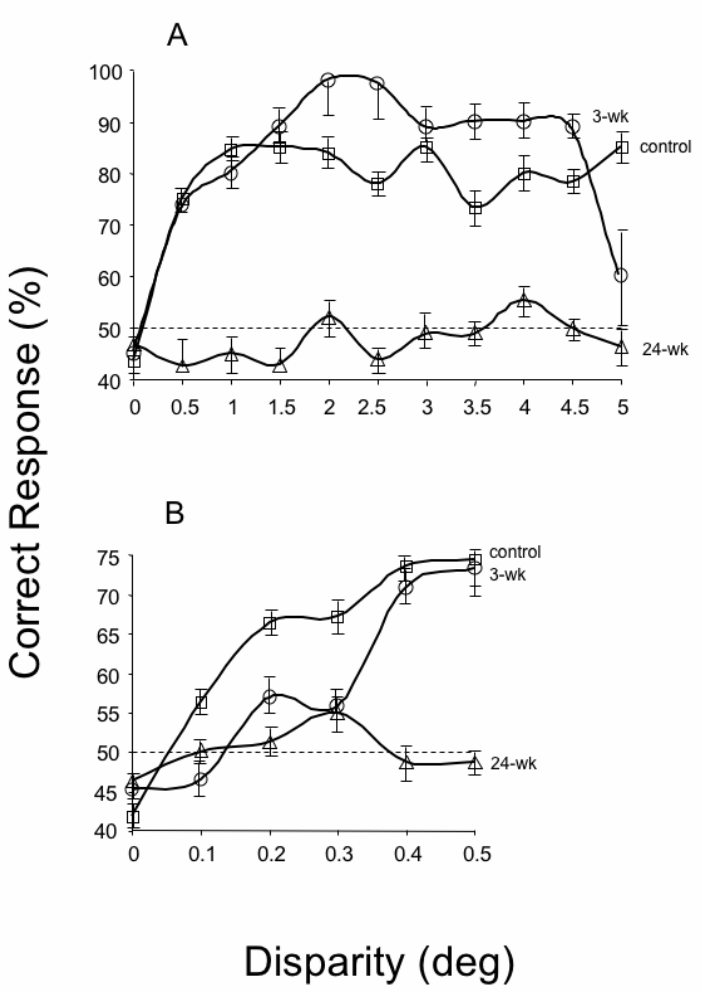

FIGURE 21

Random-dot stereopsis for crossed (+) disparities 0.1º to 5º. The control (n = 2) and 3-wk (n = 2) monkeys showed comparable levels of stereopsis at disparities 0.4º or greater. The 24-wk (n = 3) monkeys were stereoblind. Esotropic monkeys tested with prisms to realign the visual axes. 50% dashed line = chance level of performance**.** Means ± SD.

NEUROANATOMIC CONNECTIONS BETWEEN ODCS IN AREA V1

Afferents from each eye in normal primates are segregated in monocular lamina of the lateral geniculate nuclei and remain monocularly segregated at the input layer (4C) of ODCs of the striate cortex, or visual area V1.[8,9] Binocular processing is made possible by horizontal connections between right and left eye ODCs, above and below layer 4C (Figure 4),[8,57,81,82] ie, in V1 layers 4B, 2/3, and 5/6. Connections were analyzed in the 3-wk, 12-wk, and 24-wk monkeys to determine if abnormal binocular behaviors were related systematically to abnormal V1 connections. (The preceding "Results" document that the behavior of the 3-wk animals was indistinguishable from controls in almost all behavioral measures. Previous anatomic work from the author's laboratory has quantified V1 connectivity in normal primates. For this reason, neuroanatomic analysis was not repeated in the control monkeys.)

Figure 23 shows a region of foveomacular area (ie, opercular cortex) V1 in a 3-wk monkey, viewed at low magnification, in which the neuronal tracer BDA was injected into an ODC. The section was cut tangential to the external surface of the cortex, in this case through layer 4B, providing a view equivalent to peeling away the most superficial layers of V1 to look down on the cut ends of ODCs (Figure 4). Viewed in this manner, V1 is arranged as alternating rows of right-eye and left-eye ODCs. The boundaries of these rows (identified in [^{3}H] proline labeled sections, see "Methods") are indicated by the lines. BDA produced dark, patchy labeling, densest at the injection center (marked by a "+") and reducing in intensity with increasing distance from the injection site. The dark patches, viewed at higher power (Figure 23), were produced by clusters of labeled pyramidal-neuron bodies and their horizontal, axonal projections. Distal axonal projections, connecting to neurons within the injected ODC, had taken up the BDA label. These projections transported the BDA back (retrograde) to label their neuron bodies in neighboring ODCs. Neurons in immediately neighboring ODCs have the richest plexus of interconnections, accounting for the fall-off of labeled neurons with increasing distance from the injected ODC.

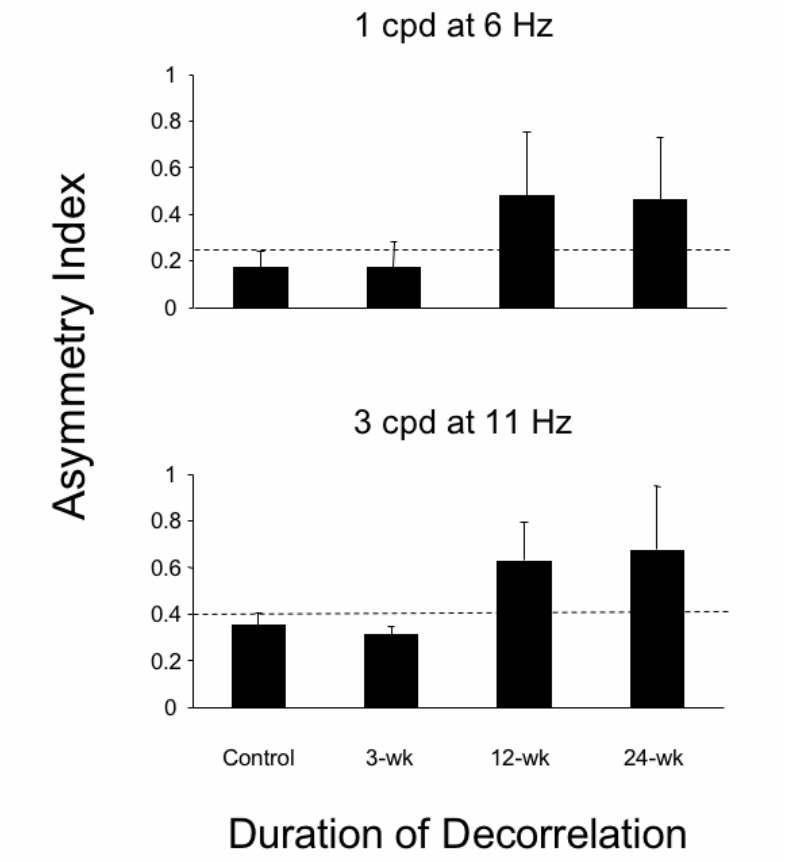

FIGURE 22

Motion visual evoked potential asymmetry indices in the 4 groups of monkeys. For 1 cpd at 6 Hz stimulus, dashed line = 0.25 upper boundary of normal. For 3 cpd at 11 Hz stimulus, dashed line = 0.40 upper boundary of normal. Pooled data for viewing with right and left eye in each animal. Mean ± SD.

To quantify precisely binocular vs monocular connections, counts of labeled pyramidal neurons were obtained from representative BDA injections in V1 layer 4B of the 3-wk monkey (SY) and the 24-wk monkey (EY). Labeled neurons were counted within the injected ODC, and within neighboring ODCs, up to 5 to 7 ODC rows (2.25 to 3.15 mm) away from the injected ODC. The results of this analysis are tabulated in the bar graphs of Figure 24, with distance from the injected ODC (number 0) annotated as increasing ODC number (1 to 7) along the x axis. The 24-wk monkey had more labeled neurons within ODCs of the same ocularity as the injected ODC, and fewer labeled neurons within ODCs of opposite ocularity, ie, neurons making monocular connections substantially

outnumbered neurons making binocular connections (*t* test for paired samples, n = 1576, comparing same to opposite ODCs, *P* = 0.004). The imbalance of monocular neurons over binocular neurons, so evident in the 24-wk monkey, was not evident in V1 of the 3-wk monkey (Figure 24). Counts of labeled neurons in the 3-wk revealed equivalent numbers within ODCs of the same vs opposite ocularity (*t* test for paired samples, n = 1365, *P* = 0.35).

Counting of labeled neurons revealed a relationship between the overall pattern of BDA-labeling, viewed at low power in individual sections, and the neuron counts (see "Methods"). When the pattern appeared as a "sunburst" distribution of label across ODCs (ie, an oval, densest at the injection center and diminishing uniformly in intensity of labeling with increasing distance from the center), counts tended to show comparable numbers of labeled neurons in right vs left eye ODCs. The "sunburst" pattern of labeling was therefore designated the "binocular connection" pattern. Alternatively, when the pattern appeared as a "skipping" distribution of label across ODCs (also densest at the center but fluctuating in intensity of labeling across every other row of ODCs), counts tended to show higher numbers of labeled neurons in ODCs which had the same ocularity as the injected ODC, and lower numbers of labeled neurons in the ODCs of opposite ocularity. The "skipping" pattern of labeling was therefore designated the "monocular connection" pattern.

Figure 25 shows these dichotomous labeling patterns for 8 representative V1 injections: 4 of the "binocular/sunburst" variety in the 3-wk monkeys (left column) and 4 of the "monocular/skipping" variety in the 12- and 24-wk animals (right column). Each injection in V1 of both cerebral hemispheres was scored as sunburst vs skipping for each of the 3-, 12-, and 24-wk monkeys (Figure 26). The most common pattern of neuronal labeling observed in the 3-wk monkeys was "sunburst/binocular," accounting for 56% of the injections (n = 19). These results are comparable to those reported previously for BDA injections in V1 layers 2, 3, and 4B of normal, adult monkeys. The lowest proportion of "sunburst/binocular" (13%) was found in the monkeys with the most severe behavioral signs of infantile strabismus—the 24-wk animals (n = 22). The 12-wk animals, who had behavioral signs intermediate between the 3- and 24-wk groups, had a proportion of "sunburst/binocular" injections (n = 16) intermediate (38%) between the 3- and 24-wk groups. These proportions differed significantly between groups (proportions test, *P* = .03).

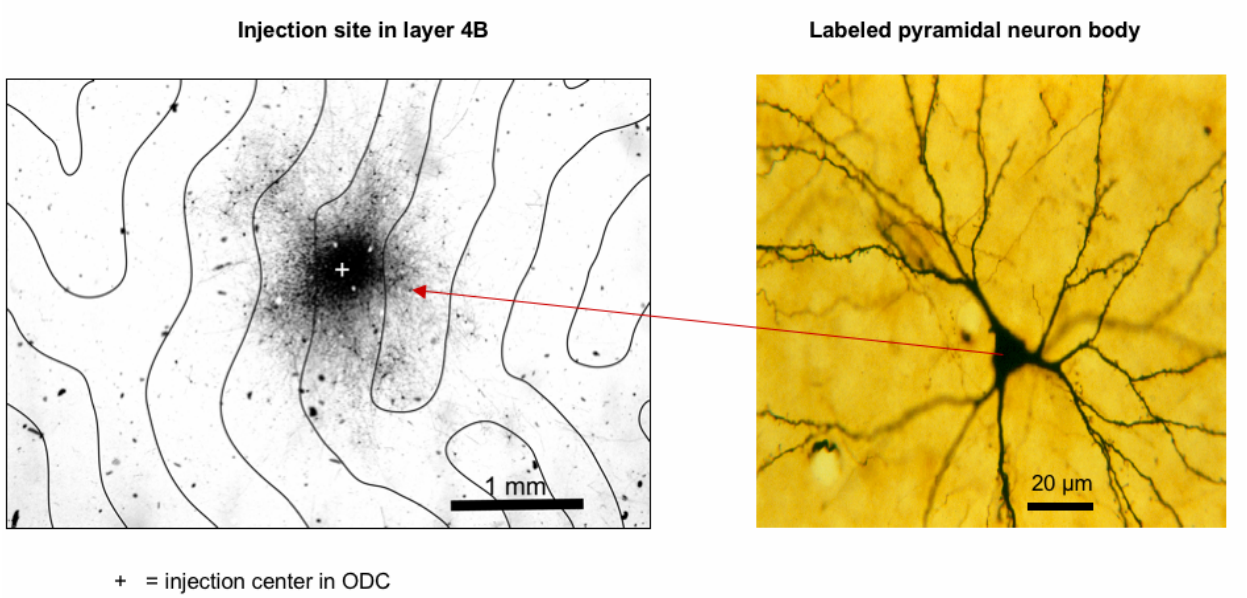

FIGURE 23

Biotinylated-dextran-amine injection site in V1 layer 4B of a 3-wk monkey, viewed at low power. Left, The center of the injection (+) stained darkly due to the high density of labeled neurons. Label intensity diminishes with increasing distance from the center in a fairly uniform fashion, ie, the number of labeled neurons decreases. Horizontal axonal connections (projections) are visible as fiber patches, radiating from the site of injection. Lines = boundaries of right-eye and left-eye ocular dominance columns (ODC), as determined by overlay of an adjacent [^{3}H]proline-labeled section through layer 4C. Right, Inset shows a labelled pyramidal neuron body viewed at higher power, and its axonal horizontal projections, in an ODC a distance from the injection site. Section (40 µm thick) cut tangential to the pial surface.

TREND OF BEHAVIORAL AND NEUROANATOMIC DEFICITS

Figure 27 plots—in a single, summarizing graph—the magnitude of each behavioral deficit as a function of increasing duration of decorrelation. The severity of the binocular-connection deficit in V1 is also plotted for comparison. Units along the y-axis are multiples of standard deviation, normalized to the performance of the 3-wk monkey group. The purpose here is not to connote perfect

concordance, one deficit to another, but to illustrate that (1) all behaviors worsened with prolonged durations and (2) as V1 binocularity worsened, behaviors worsened progressively.

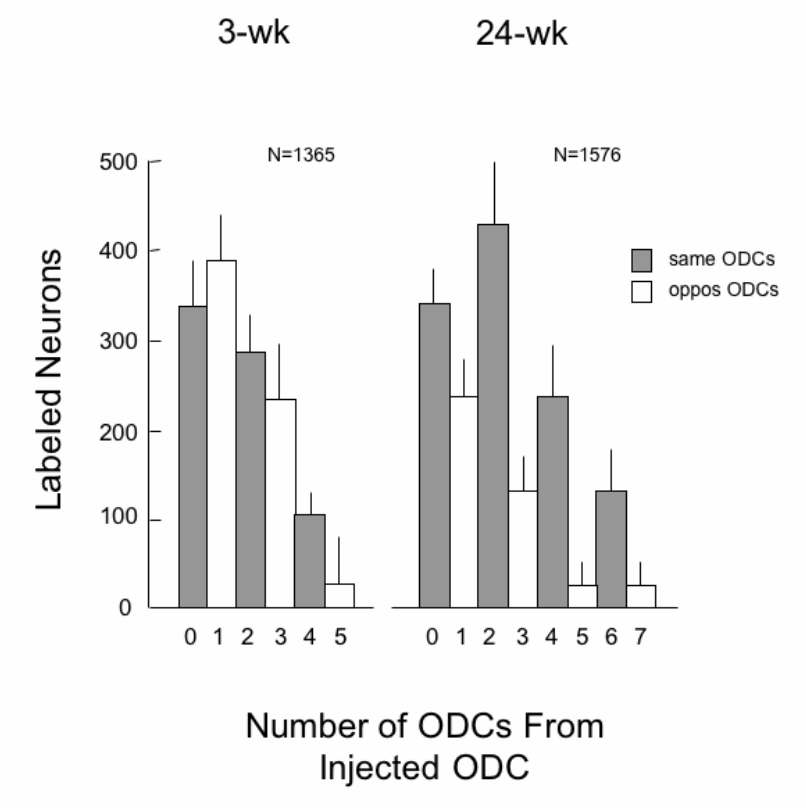

FIGURE 24

Number of labeled pyramidal neuron bodies in same-eye and opposite-eye ocular dominance columns (ODCs) of V1 after injection into a single ODC, 3-wk vs 24-wk monkey. The injected ODC is at zero on the x-axis, and neighboring ODCs are numbered in successive rows from the injected ODC. V1 of the 3-wk monkey had equivalent numbers of labeled neurons in same and opposite-eye ODCs within 4 rows from the injection site (*t* test, $P = .15$, comparing ODC 0 to ODC 1; 2 to 3). Fewer neurons were labeled by the transported tracer—in both same and opposite-eye ODCs—with increasing distance from the injected ODC. In the 24-wk monkey, greater numbers of labeled neurons in same-eye, and fewer in opposite-eye ODCs within 4-or-more rows from the injection site (*t* test, $P = .03$, comparing ODC 0 to ODC 1; 2 to 3). Means ± SD.

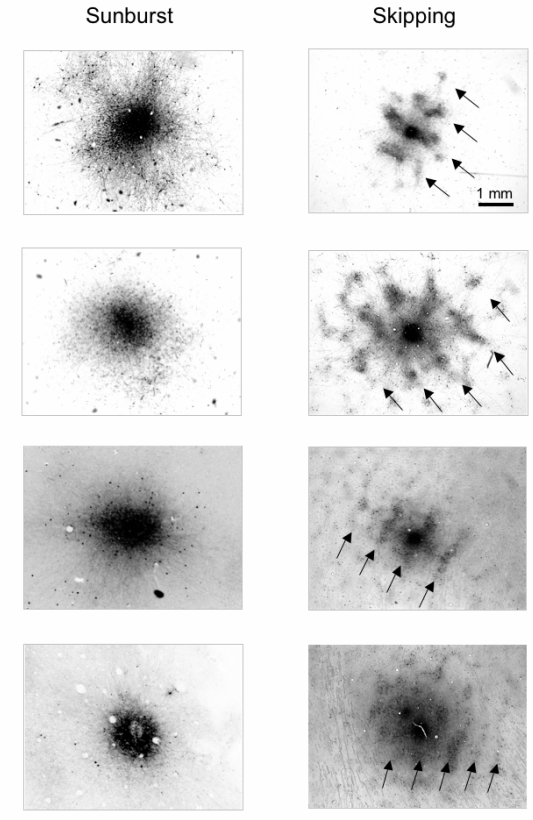

FIGURE 25

Biotinylated-dextran-amine (BDA) injection sites in V1 layer 4B viewed at lower power. Four "sunburst" (binocular) patterns of labeling, in control and 3-wk monkeys; and 4"skipping" (monocular) patterns in the 12- and 24-wk monkeys. Arrows in the "skipping" patterns indicate same-eye ocular dominance columns (ODCs; every-other-row of ODCs) labeled more intensely at low-power, corresponding to greater numbers of labeled neurons when viewed at higher-power. Sections (40 μm thick) cut tangential to the pial surface.

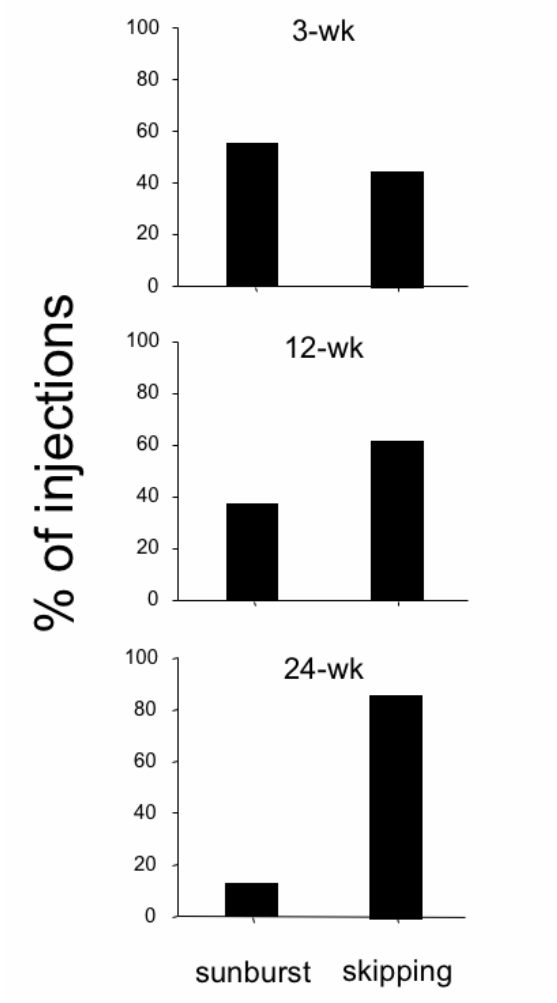

FIGURE 26

Proportion of V1 injections that corresponded to "sunburst" (binocular) vs "skipping" (monocular) patterns of transported label in the 3-wk, 12-wk, and 24-wk monkeys. Pooled data within groups for multiple injections into both V1 hemispheres.

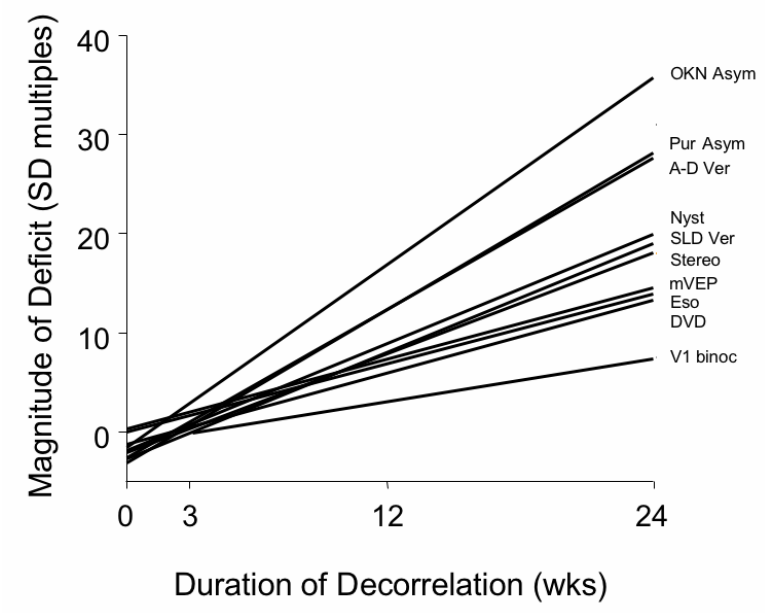

FIGURE 27

Severity of behavioural and neuroanatomic deficit with increasing duration of binocular decorrelation. For the behavioural measures, the regression lines plot the magnitude of the deficit in multiples of standard deviation, normalized to the average value of the 3-wk monkey group. For the neuroanatomic measure, the line plots magnitude as a multiple of the proportion difference in the 3-wk monkey group. OKN Asym, OKN nasotemporal asymmetry; Pur Asym, pursuit asymmetry; A-D Ver, accommodative-disparity vergence; Nyst, latent nystagmus; SLD Ver, short-latency disparity vergence; Stereo, stereopsis; mVEP, motion VEP; Eso, esotropia; DVD, dissociated vertical deviation; V1 binoc, V1 binocular connections.

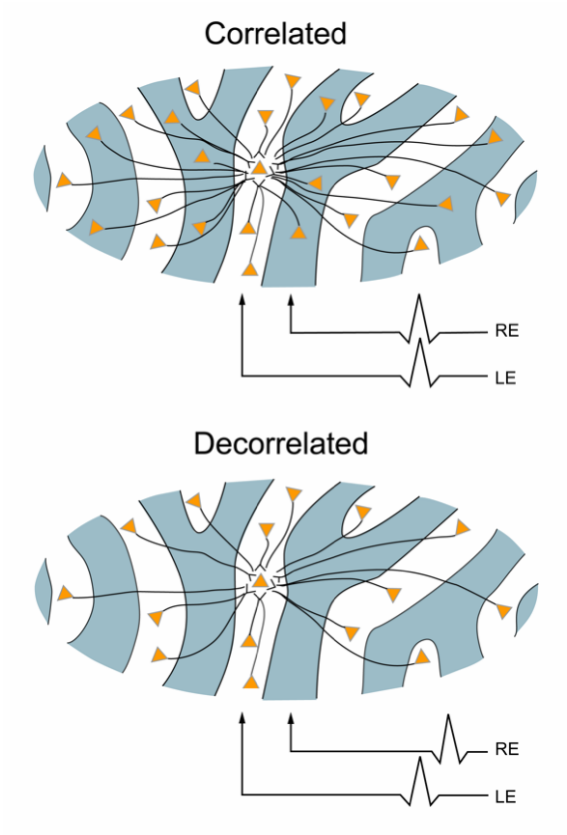

FIGURE 28

Horizontal axonal connections between same- and opposite-eye ocular dominance columns caused by correlated and decorrelated binocular input during an early critical period. Correlated activity ("cells that fire together, wire together") stabilizes immature binocular connections, resulting in equivalent numbers of monocular/same-eye and binocular/opposite-eye connections. Decorrelated activity punishes immature binocular connections ("cells that fire apart, depart") resulting in a paucity of binocular, but retained monocular connections.

DISCUSSION

The purpose of this study was to answer 2 major questions. First, can esotropia be produced reliably in normal infant primates by imposing binocular decorrelation during an early critical period for visuomotor development? The answer to this question is yes. Each animal exposed to binocular decorrelation by prism-dissociation in the first weeks of life developed concomitant esotropia. In the animals exposed to longer durations of decorrelation, the esotropia was accompanied by a constellation of sensory and motor signs mimicking closely the features observed in strabismic children. Second, does the severity of the signs increase systematically as a function of duration of decorrelation? The answer to this question is also yes; the magnitude of each behavioral and anatomic abnormality tended to increase—often monotonically—with longer decorrelation duration. These data provide information that would be difficult or impossible to obtain from human infants in randomized clinical trials. Using a primate model allowed us to impose precise periods of deprivation, to then record—in hundreds of quantitative, machine-like trials—the resultant behavioral deficits, and to then analyze, at a level of detail unobtainable by any current neuroimaging technique in human, the underlying neural circuitry.

IMPEDING MATURATION OF FUSION AND CONVERGENT BIASES

Behavioral studies have shown that the postnatal development of binocular sensory and motor functions in normal infant monkeys parallels that of normal infant humans, but on a compressed time scale; 1 week of monkey development approximates 1 month of human.[48,52,83,84] Binocular disparity sensitivity and binocular fusion are absent in both human and monkey neonates. Stereopsis emerges abruptly in human during the first 3 to 5 months of postnatal life,[85-89] and in monkey during the first 3 to 5 weeks,[48] achieving adultlike levels of sensitivity.

Fusional vergence eye movements in neonates are also immature, maturing during an equivalent period. In the first 2 months of life, alignment is unstable in human infants and responses to step or ramp changes in disparity are inaccurate, favoring overconvergence.[90-93] Transient convergence errors exceed divergence errors by a ratio of 4:1. The fusional vergence response to crossed (convergent) disparity is also intact earlier and substantially more robust than that to divergent disparity. The innate bias favoring convergence persists after full maturation of binocular disparity sensitivity. Fusional convergence ranges in normal, adult primates exceed divergence ranges by a mean ratio of 2:1,[94,95] and brainstem premotor convergence neurons outnumber divergence neurons by a ratio of 3:2.[96,97]

Maturation of fusional vergence was impaired in the current study by imposing binocular decorrelation throughout the first weeks of life. Vergence decompensated to esotropia in each animal, without manipulation of the extraocular muscles or motor pathways. The magnitude of the esotropia increased as a function of decorrelation duration. These results imply that esotropia is an expression of an innate, convergence bias. The convergence bias is held in check by maturation of disparity vergence but may be expressed during an

early period of vergence instability by impeding cortical connections that mediate disparity sensitivity. The longer these connections are impeded, the more the convergence bias is expressed.

NASALWARD BIASES OF MOTION PERCEPTION AND CONJUGATE GAZE

The nasalward bias of the vergence pathway in normal primates has analogs in the visual processing of horizontal motion, both for perception and conjugate eye tracking. In the first months of life in human and weeks of life in monkey, monocular motion VEPs reveal a nasotemporal asymmetry[45,51,79,98]; monocular forced preferential looking testing reveals greater perceptual sensitivity to nasalward motion[99]; and monocular pursuit and optokinetic tracking reveal biases favoring nasalward target motion.[83,100-103] These nasalward motion biases are pronounced before onset of sensorial fusion and stereopsis, but systematically diminish thereafter. If normal maturation of binocularity is impeded by eye misalignment or monocular deprivation, the nasalward biases persist and may become more pronounced.[80,99,104-109]

The results reported here reinforce and extend these findings by demonstrating a relationship between the duration of binocular decorrelation and the severity of nasotemporal asymmetries. The animals that retained (control monkeys) or regained (3-wk monkeys) binocular fusion showed symmetric nasotemporal responses. The animals that lost binocular fusion (the 12-wk and the 24-wk monkeys) showed pronounced asymmetries. In these animals, NBIs for both smooth pursuit and OKN increased as the duration of decorrelation increased, as did the asymmetry indices for motion VEPs.

DECORRELATED INPUT AND LOSS OF V1 BINOCULAR CONNECTIONS

V1 horizontal, axonal connections may play a central role in the causation and signs of infantile esotropia. Binocularity in primates begins with horizontal connections between V1 ODCs of opposite ocularity.[8,57,110] These connections are immature in the first weeks of life, conveying crude, weak binocular responses.[111-113] Maturation of binocular connections requires correlated (synchronous) activity between right-eye and left-eye geniculostriate inputs (Figure 28).[114,115] Decorrelation of inputs, produced by binocular noncorrespondence, causes loss of horizontal connections over a period of days in V1 of kittens.[114,116] The inference from the current results is that the loss occurs over a period of weeks in V1 of monkeys.

These experiments in monkeys show that *extrinsically imposed* binocular decorrelation causes loss of V1 binocular connections, and esotropia. Could *intrinsically generated* decorrelation cause an analogous loss in some human infants? Several lines of evidence suggest so. The correlated signals that stabilize horizontal connections must flow through immature, monocular geniculostriate fibers. These fibers in infants are vulnerable to cytotoxic insults from a variety of causes,[117-119] and perinatal insults to the geniculostriate pathways are linked strongly to subsequent onset of strabismus.[13-16] Periventricular hemorrhage increases the prevalence of infantile strabismus 50- to 100-fold. Nonspecific cerebral insults, eg, from very low birth weight, increase the risk 20- to 30-fold.[14,120] Apart from cytotoxic injury, normal inequalities of geniculostriate development promote intrinsic binocular decorrelation. In V1 of each hemisphere, projections from the ipsilateral eye (temporal hemiretina) are slower to develop and smaller in number than projections from the contralateral eye (nasal hemiretina).[121]Any perturbation that slowed geniculostriate development would prolong the duration of binocular decorrelation caused by this input inequality. The decorrelation mechanism is appealing because it is parsimonious: a simple, "final common pathway" origin for essential infantile esotropia. The "essential" factors that perturb oligodendrocytes or delay ipsilateral projections could be quite subtle, varying idiosyncratically with individual thresholds from one strabismic infant to another, eg, genetically expressed neurotrophins, gestational nicotine exposure, and mild toxemia.

PAUCITY OF BINOCULAR V1 CONNECTIONS AND IMPAIRED DISPARITY-SENSITIVITY

The esotropic monkeys were able to generate accommodative vergence and normal saccadic eye movements, yet displayed striking maldevelopments of binocular-disparity induced vergence. These results imply that the neural mechanism of the disparity vergence deficit is not in the extraocular muscles, motor nuclei, or convergence-related neurons of the midbrain, but rather in the visual cortical areas that process disparity early in the vergence sensorimotor pathway. Disparity-selective neurons implicated in the control of vergence have been found in visual areas V1, V2, MT, and MST in monkey and fall generally into "near" and "far" subtypes, sensitive to crossed and uncrossed disparities, respectively, that could drive convergence and divergence.[10,122-125] Patterns containing binocular disparity act as a powerful stimulus to vergence in both humans and monkeys, even if the patterns cannot evoke a percept of binocular fusion because they are composed of anticorrelated dots.[11] Taken together, these findings imply that vergence is driven by disparity-sensitive neurons at the earliest (ie, prestereoscopic) stage of binocular processing—visual area V1.

The 12- and 24-wk esotropic monkeys of the current study had a paucity of V1 layer 4B horizontal connections joining ODCs of opposite ocularity. The output from layer 4B provides a major projection to extrastriate areas MT/MST, which mediate perception of stereopsis and help modulate vergence.[125-129] The missing V1 binocular connections in these animals provide a structural explanation for their deficient disparity-vergence and stereopsis behaviors. Although binocular functions were lost, the esotropic monkeys retained normal monocular (grating) visual acuity in each eye. The lack of horizontal connections between opposite-eye ODCs would not be expected to impair monocular spatial vision, since the monkeys would retain connections between orientation-tuned neurons [130,131] belonging to the same eye.

Our finding that 56% of labeled injections were binocular in the 3-wk repair monkeys is within the lower range found in normal adult animals. Anatomic labeling of binocular connections corresponds roughly but not strictly to binocular responsiveness measured by electrophysiolgical methods. In normal adult primates, ~ 80% of V1 neurons show some binocular responsiveness, but only 55% to 75% of V1 neurons labeled anatomically show distinct binocular connectivity.[57] This functional-structural discrepancy suggests that

some binocular connections, too faint to allow unambiguous anatomic detection using the methods we employed, are sufficient nonetheless to elicit a weak binocular response using extracellular recording.

PAUCITY OF BINOCULAR V1 CONNECTIONS AND NASO-TEMPORAL GAZE ASYMMETRIES

The nasally directed asymmetries of pursuit and OKN, as well as the nasal drifts of latent fixation nystagmus, appear to be generated by a directional bias encoded within the immature, conjugate gaze pathways of the visual cortex, in particular, visual areas V1, MT, and MST. The mechanism for this nasal bias has been elucidated by electrophysiologic and anatomic studies[25,132-136] and summarized in a neural circuit model.[6,25] In brief, the pursuit/OKN premotor neuron area of extrastriate cortex (area MST)—in each cerebral hemisphere— is innately wired so as to receive downstream input from visual motion neurons (of areas V1/MT) that command nasally directed pursuit. This innate wiring is *monocular*; binocular visual connections are not required. However, the V1/MT neurons that command temporally directed pursuit gain access to area MST predominantly through *binocular* connections. If binocularity fails to develop, the system will be incapable of activating normal, temporally directed pursuit.[25,106,107,135] The innate, monocular-nasal bias is also evident in the population of MST neurons that encode gaze-holding,[132,137] manifested as latent fixation nystagmus with nasal slow-phase drifts of eye position. The results of the current study reinforce the validity of this gaze-asymmetry model. The severity of the pursuit/OKN asymmetries, and the severity of latent nystagmus, increased systematically with loss of binocular connections in V1.

IMPLICATIONS FOR EARLY STRABISMUS REPAIR IN HUMAN INFANTS

The timing of surgical corrections for esotropia in human infants is controversial.[22,138,139] In North America, the mean age at surgical repair ranges from 10 to 18 months,[26,139] and in many parts of western Europe, surgical repair is delayed to age 2 to 4 years.[140] Stereopsis is restored in only 40% to 50% of infants operated on at age 10 to 18 months, and seldom to normal threshold levels.[47,141] Advances in outpatient infant anesthesia and surgical technique have made it possible to realign the eyes of strabismic children at weeks or months of age. The fusion and stereopsis outcomes of infants who have had "early" surgery (at or before age 4 to 6 months) appear to be better than those in the delayed surgery groups.[17,18,20,142]

Critics of early surgery argue that the esotropia may have resolved spontaneously in infancy if left untreated. The Congenital Esotropia Observational Study found that the strabismus in fact persisted in 98% of infants who had large-magnitude (≥ 40 prism diopters) constant esotropia.[143,144] A follow-up study of infants with smaller, variable-angle esotropia found that surprisingly few convert to normal fusion behaviors.[145] Even small, early-onset, constant esotropias tend predominantly to progress to larger-magnitude angles of misalignment.

Early surgery in humans is believed to enhance sensory outcomes by re-establishing correlated binocular activity during an early critical period for the development of stereopsis.[20,86,146] Although both age at alignment and duration of misalignment are correlated with long-term stereoacuity outcome, the duration of misalignment appears to be the more important factor.[20,146] Durations less than a total of 3 months are associated with good to excellent restoration of stereopsis and motor fusion. The results of the current study provide indirect support for early surgery by showing that a wide range of fusional visuomotor behaviors, and the underlying V1 binocular circuitry, can be repaired in a primate model. The repair was effective when the duration of binocular decorrelation was limited to the human-equivalent of ~3 months.

ACKNOWLEDGMENTS

Funding/Support: Supported by the National Institutes of Health grant 5R01 EY010214 08-11 from the National Eye Institute and a Research to Prevent Blindness Walt and Lilly Disney Scholars Award for Amblyopia Research.

Financial Disclosure: None.

Other Acknowledgments: We are indebted to Mae Gordon, PhD, Director of the Biostatistics Core, Department of Ophthalmology and Visual Sciences, Washington University School of Medicine, for assistance with statistical analysis. Paul Foeller, MS (Washington University), provided invaluable help with all aspects of animal training, eye movement recording, and neuroanatomic preparation. Dolores Bradley, PhD, (Yerkes Primate Center, Atlanta, Georgia) directed the initial animal rearing. Andreas Burkhalter, PhD, assisted with all phases of the neuroanatomic work. Agnes Wong, MD, PhD, (Washington University and University of Toronto) assisted with eye movement analysis, as did Michael Richards, BS, Leo Sin, BS, and Aasim Hasany, BS (all of the University of Toronto).

REFERENCES

1. Graham PA. Epidemiology of strabismus. *Br J Ophthalmol* 1974;58:224-231.
2. Rubenstein RS, Lohr KN, Brook RH, Goldberg GA, Kamberg CJ. *Measurement of Physiological Health for Children, Vol 4. Vision Impairments*. Santa Monica, CA: Rand Corporation; 1985.
3. Lorenz B. Genetics of isolated and syndromic strabismus: facts and perspectives. *Strabismus* 2002;10:147-156.
4. US Department of Health, Education, and Welfare. Eye examination findings among children. *Nat Health Surv* 1972;11:1-47.
5. Kiorpes L, Boothe RG, Carlson MR, Alfi D. Frequency of naturally occurring strabismus in monkeys. *J Pedriatr Ophthalmol Strabismus* 1985;22:60-64.
6. Tychsen L. Strabismus: the scientific basis. In: Taylor D, Hoyt CS, eds. *Pediatric Ophthalmology and Strabismus*. 3rd ed. Edinburgh: Elsevier Saunders; 2005:836-848.

7. Narasimhan A, Tychsen L, Poukens V, Demer JL. Horizontal rectus muscle anatomy in naturally and artificially strabismic monkeys. *Invest Ophthalmol Vis Sci* 2007;48:2576-2588.
8. Hubel DH, Wiesel TN. Ferrier lecture. Functional architecture of macaque monkey visual cortex. *Proc R Soc Lond [Biol]* 1977;198:1-59.
9. Hubel DH. Exploration of the primary visual cortex, 1955-78. *Nature* 1982;299:515-524.
10. 10. Poggio GF, Fischer B. Binocular interaction and depth sensitivity in striate and prestriate cortex of behaving rhesus monkey. *J Neurophysiol* 1977;40:1392-1405.
11. Masson GS, Busettini C, Miles FA. Vergence eye movements in response to binocular disparity without depth perception. *Nature* 1997;389:283-286.
12. Cumming BG, Parker AJ. Binocular neurons in V1 of awake monkeys are selective for absolute, not relative, disparity. *J Neurosci* 1999;19:5602-6218.
13. Tamura EE, Hoyt CS. Oculomotor consequences of intraventricular hemorrhages in premature infants. *Arch Ophthalmol* 1987;105:533-535.
14. van Hof-van Duin J, Evenhuis-van Leunen A, Mohn G, Baerts W, Fetter WPF. Effects of very low birth weight (VLBW) on visual development during the first year after term. *Early Hum Dev* 1989;20:255-266.
15. Pike MG, Holmstrom G, de Vries LS, et al. Patterns of visual impairment associated with lesions of the preterm infant brain. *Dev Med Child Neurol* 1994;36:849-862.
16. Hoyt CS. Visual function in the brain-damaged child. *Eye* 2003;17:371-386.
17. Ing M, Costenbader FD, Parks MM, Albert DG. Early surgery for congenital esotropia. *Am J Ophthalmol* 1966;61:1419-1427.
18. Wright KW, Edelman PM, McVey JH, Terry AP, Lin M. High-grade stereo acuity after early surgery for congenital esotropia. *Arch Ophthalmol* 1994;112:913-919.
19. Ing MR. Outcome study of surgical alignment before six months of age for congenital esotropia. *Ophthalmology* 1995;102:2041-2045.
20. Birch EE, Fawcett S, Stager DR. Why does early surgical alignment improve stereopsis outcomes in infantile esotropia? *J AAPOS* 2000;4:10-14.
21. Tychsen L. Can ophthalmologists repair the brain in infantile esotropia? Early surgery, stereopsis, monofixation syndrome, and the legacy of Marshall Parks. *J AAPOS* 2005;9:510-521.
22. Parks MM. Operate early for congenital strabismus. In: Brockhurst RJ, Boruchoff SA, Hutchinson BT, et al, eds. *Controversy in Ophthalmology*. Philadelphia: WB Saunders; 1977:423-430.
23. Costenbader FD. Infantile esotropia. *Trans Am Ophthalmol Soc* 1961;59:397-429.
24. Parks M, Wheeler M. Concomitant esodeviations. In: Duane T, Jaeger E, eds. *Clinical Ophthalmology.* Vol 1. Philadelphia: Harper and Row; 1987:chap 12.
25. Tychsen L. Infantile esotropia: current neurophysiologic concepts. In: Rosenbaum AL, Santiago AP, eds. *Clinical Strabismus Management*. Philadelphia: WB Saunders; 1999:117-138.
26. von Noorden GK. A reassessment of infantile esotropia. XLIV Edward Jackson Memorial Lecture. *Am J Ophthalmol* 1988;105:1-10.
27. Crawford MLJ, von Noorden GK. Optically induced concomitant strabismus in monkeys. *Invest Ophthalmol Vis Sci* 1980;19:1105-1109.
28. Crawford M. Optical control of early visual experience in monkeys. *Behav Brain Res* 1996;79:201-205.
29. Foeller P, Tychsen L. Eye movement training and recording in alert macaque monkeys: 1. Operant visual conditioning 2. Magnetic search coil and head restraint surgical implantation 3. Calibration and recording. *Strabismus* 2002;10:5-22.
30. Norcia AM, Tyler CW. Spatial frequency sweep VEP: visual acuity during the first year of life. *Vision Res* 1985;25:1399-1408.
31. Norcia AM. Vision testing by visual evoked potential techniques. In: Isenberg SJ, ed. *The Eye in Infancy*. 2nd ed. St Louis: Mosby - Year Book, Inc; 1994:157-173.
32. Wong AMF, Tychsen L. Effects of extraocular muscle tenotomy on congenital nystagmus in macaque monkeys. *J AAPOS* 2002;6:100-107.
33. Robinson DA. A method of measuring eye movement using a scleral search coil in a magnetic field. *IEEE Trans Biomed Eng* 1963;10:137-145.
34. Fuchs AF. Saccadic and smooth pursuit eye movements in the monkey. *J Physiol* 1967;191:609-631.
35. Scott C, Gumdrop G, Tychsen L. Automated cover test for eye misalignment in awake monkeys using spectacle-mounted liquid crystal shutters. *Binocul Vis Strabismus Q* 1999;15:59-66.
36. Quick MW, Boothe RG. Measurement of binocular alignment in normal monkeys and in monkeys with strabismus. *Invest Ophthalmol Vis Sci* 1989;30:1159-1168.
37. von Noorden GK. *Binocular Vision and Ocular Motility*. St Louis: Mosby - Year Book, Inc; 1996.
38. Rashbass C. The relationship between saccadic and smooth tracking eye movements. *J Physiol* 1961;159:326-338.
39. Lisberger SG, Westbrook LE. Properties of visual inputs that initiate horizontal smooth pursuit eye movements in monkeys. *J Neurosci* 1985;5:1662-1673.
40. Leigh RJ, Zee DS. *The Neurology of Eye Movements*. New York: Oxford University Press; 1999.

41. Busettini C, Miles FA, Krauzlis RJ. Short-latency disparity vergence responses and their dependence on a prior saccadic eye movement. *J Neurophysiol* 1996;75:1392-1410.
42. Tychsen L, Scott C. Maldevelopment of convergence eye movements in macaque monkeys with small and large-angle infantile esotropia. *Invest Ophthalmol Vis Sci* 2003;44:3358-3368.
43. Teller DY. The forced-choice preferential looking procedure: a psychophysical technique for use with human infants. *Infant Behav Dev* 1979;2:135-153.
44. Teller DY, Regal DM, Videen TO, Pulos E. Development of visual acuity in infant monkey (*Macaca nemestrina*) during early postnatal weeks. *Vision Res* 1978;18:561-566.
45. Norcia AM, Garcia H, Humphry R, Holmes A, Hamer RD, Orel-Bixler D. Anomalous motion VEPs in infants and in infantile esotropia. *Invest Ophthalmol Vis Sci* 1991;32:436-439.
46. Norcia AM. Improving infant evoked response measurement. In: Simons K, ed. *Early Visual Development, Normal and Abnormal*. New York: Oxford University Press; 1993:536-552.
47. Birch EE, Stager DR, Everett ME. Random dot stereoacuity following surgical correction of infantile esotropia. *J Pediatr Ophthalmol Strabismus* 1995;32:231-235.
48. O'Dell C, Boothe RG. The development of stereoacuity in infant rhesus monkeys. *Vision Res* 1997;37:2675-2684.
49. Cornsweet TN. The staircase-method in psychophysics. *Am J Psychol* 1962;175:485-491.
50. Victor J, Mast J. A new statistic for steady-state evoked potentials. *Electroenceph Clin Neurophysiol* 1991;78:378-388.
51. Norcia AM. Abnormal motion processing and binocularity: infantile esotropia as a model system for effects of early interruptions of binocularity. *Eye* 1996;10:259-265.
52. Brown RJ, Wilson JR, Norcia AM, Boothe RG. Development of directional motion symmetry in the monocular visually evoked potential of infant monkeys. *Vision Res* 1998;38:1253-1263.
53. Tychsen L, Yildirim C, Anteby I, Boothe R, Burkhalter A. Macaque monkey as an ocular motor and neuroanatomic model of human infantile strabismus. In: Lennerstrand G, Ygge J, eds. *Advances in Strabismus Research: Basic and Clinical Aspects.* Vol 78. London, UK: Wenner-Gren International Series, Portland Press Ltd; 2000:103-119.
54. Tychsen L, Wong AMF, Foeller P, Bradley D. Early versus delayed repair of infantile strabismus in macaque monkeys: II. Effects on motion visually evoked responses. *Invest Ophthalmol Vis Sci* 2004;45:821-827.
55. Horton JC, Hocking DR. An adult-like pattern of ocular dominance columns in striate cortex of newborn monkeys prior to visual experience. *J Neurosci* 1996;16:1791-1807.
56. Horton JC, Hocking DR. Intrinsic variability of ocular dominance column periodicity in normal macaque monkeys. *J Neurosci* 1996;16:7228-7339.
57. Tychsen L, Wong AMF, Burkhalter A. Paucity of horizontal connections for binocular vision in V1 of naturally-strabismic macaques: cytochrome-oxidase compartment specificity. *J Comp Neurol* 2004;474:261-275.
58. Wong AMF, Burkhalter A, Tychsen L. Suppression of metabolic activity caused by infantile strabismus and strabismic amblyopia in striate visual cortex of macaque monkeys. *J AAPOS* 2005;9:37-47.
59. Wiesel TN, Hubel DH. Ordered arrangement of orientation columns in monkeys lacking visual experience. *J Comp Neurol* 1974;158:307-318.
60. Horton JC, Hocking DR, Adams DL. Metabolic mapping of suppression scotomas in striate cortex of macaques with experimental strabismus. *J Neurosci* 1999;19:7111-7129.
61. Horton JC. Cytochrome oxidase patches: a new cytoarchitectonic feature of monkey visual cortex. *Philos Trans R Soc Lond B Biol Sci* 1984;304:199-253.
62. West MJ. New stereological methods for counting neurons. *Neurobiol Aging* 1993;14:275-285.
63. Daly LE, Bourke GJ, McGilvray J, eds. Interpretation and uses of medical statistics.*Comparisons of More Than Two Groups: Analysis of Variance and the Chi-square Test.* 4th ed. Oxford: Blackwell Scientific Publications; 1991.
64. Walsh JE. *Handbook of Nonparametric Statistics*. Princeton, NJ: D.Van Nostrand Company; 1968.
65. Helveston EM. Dissociated vertical deviation—a clinical and laboratory study. *Trans Am Opthalmol Soc* 1981:734-779.
66. Guyton DL, Cheeseman EW, Ellis FJ, Straumann D, Zee DS. Dissociated vertical deviation: an exaggerated normal eye movement used to damp cyclovertical latent nystagmus. *Trans Am Ophthalmol Soc* 1998;96.
67. Wilson ME, McClatchey SK. Dissociated horizontal deviation. *J Pediatr Ophthalmol Strabismus* 1991;28:90-95.
68. Zubcov AA, Reinecke RD, Calhoun JH. Asymmetric horizontal tropias, DVD, and manifest latent nystagmus: an explanation of dissociated horizontal deviation. *J Pediatr Ophthalmol Strabismus* 1990;27:59-65.
69. Healy MH, Symmes D, Ommaya AK. Visual discordance cues induce prism adaptation in normal monkeys. *Percept Mot Skills* 1973;37:683-693.
70. Schor CM. Fixation disparity and vergence adaptation. In: Schor CM, Ciuffreda KJ, eds. *Vergence Eye Movements: Basic and Clinical Aspects*. Boston: Butterworths; 1983:465-516.
71. Birch EE, Stager DR. Monocular acuity and stereopsis in infantile esotropia. *Invest Ophthalmol Vis Sci* 1985;26:1624-1630.
72. Birch EE, Hale LA. Criteria for monocular acuity deficit in infancy and early childhood. *Invest Ophthalmol Vis Sci* 1988;29:636-643.
73. Rubin ML. *Optics for Clinicians.* 2nd ed. Gainesville, FL: TRIAD Scientific Publishers; 1977.

74. Committee NEINIH. *A Classification of Eye Movement Abnormalities and Strabismus (CEMAS). Report of a National Eye Institute Sponsored Workshop.* Bethesda, MD: National Eye Institute, National Institute of Health; February 9-10, 2001.
75. Miles FA. Adaptive regulation in the vergence and accommodation control systems. In: Berthoz A, Melvill Jones G, eds. *Adaptive Mechanisms in Gaze Control*. Amsterdam: Elsevier; 1985:81-94.
76. Kenyon RV, Ciuffreda KJ, Stark L. Dynamic vergence eye movements in strabismus and amblyopia: symmetric vergence. *Invest Ophthalmol Vis Sci* 1980;19:60-74.
77. Cumming BG, Judge SJ. Disparity-induced and blur-induced convergence eye movement and accommodation in the monkey. *J Neurophysiol* 1986;55:896-914.
78. Ciuffreda KJ, Kenyon RV. Accommodative vergence and accommodation in normals, amblyopes, and strabismics. In: Schor CM, Ciuffreda KJ, eds. *Vergence Eye Movements: Basic and Clinical Aspects*. Boston: Butterworth Publishers; 1983:101-173.
79. Birch EE, Fawcett S, Stager D. Co-development of VEP motion response and binocular vision in normal infants and infantile esotropes. *Invest Ophthalmol Vis Sci* 2000;41:1719-1723.
80. Fawcett SL, Birch EE. Motion VEPs, stereopsis, and bifoveal fusion in children with strabismus. *Invest Ophthalmol Vis Sci* 2000;41:411-416.
81. Rockland KS, Lund JS. Intrinsic laminar lattic connections in primate visual cortex. *J Comp Neurol* 1983;216:303-318.
82. Lund JS, Yoshioka T, Levitt JB. Comparison of intrinsic connectivity in different areas of macaque monkey cerebral cortex. *Cereb Cortex* 1993;3:148-162.
83. Atkinson J. Development of optokinetic nystagmus in the human infant and monkey infant: an analogue to development in kittens. In: Freeman RD, ed. *Developmental Neurobiology of Vision.* New York: Plenum; 1979:277-287.
84. Boothe RG, Dobson V, Teller DY. Postnatal development of vision in human and nonhuman primates. *Annu Rev Neurosci* 1985;8:495-546.
85. Fox R, Aslin RN, Shea SL, Dumais ST. Stereopsis in human infants. *Science* 1980;207:323-324.
86. Birch EE, Gwiazda J, Held R. Stereoacuity development for crossed and uncrossed disparities in human infants. *Vision Res* 1982;22:507-513.
87. Birch EE, Gwiazda J, Held R. The development of vergence does not account for the onset of stereopsis. *Perception* 1983;12:331-336.
88. Birch EE, Shimojo S, Held R. Preferential-looking assessment of fusion and stereopsis in infants aged 1 to 6 months. *Invest Ophthalmol Vis Sci* 1985;26:366-370.
89. Gwiazda J, Bauer JAJ, Held R. Binocular function in human infants: correlation of stereoptic and fusion-rivalry discriminations. *J Pediatr Ophthalmol Strabismus* 1989;26:128-132.
90. Aslin RN. Development of binocular fixation in human infants. *Eye Movements: Cognition and Visual Perception*. Hillsdale, NJ: Erlbaum; 1977:31-51.
91. Aslin RN, Jackson RW. Accommodative-convergence in young infants: development of a synergistic sensory-motor system. *Can J Psychol* 1979;33:222-231.
92. Horwood AM. Maternal observations of ocular alignment in infants. *J Pediatr Ophthalmol Strabismus* 1993;30:100-105.
93. Horwood AM, Riddell PM. Can misalignments in typical infants be used as a model for infantile esotropia? *Invest Ophthalmol Vis Sci* 2004; 45:714-720.
94. Mellick A. Convergence. An investigation into the normal standards of age groups. *Br J Ophthalmol* 1949;33:755-763.
95. Tait EF. Fusional vergence. *Am J Ophthalmol* 1949;32:1223-1230.
96. Mays LE. Neurophysiological correlates of vergence eye movements. In: Schor CM, Ciuffreda KJ, eds. *Vergence Eye Movements: Basic and Clinical Aspects*. Boston: Butterworths; 1983:649-670.
97. Mays LE. Neural control of vergence eye movements: convergence and divergence neurons in midbrain. *J Neurophysiol* 1984;51:1091-1108.
98. Brown RJ, Norcia AM. A method for investigating binocular rivalry in real-time with the steady-state VEP. *Vision Res* 1997;37:1-8.
99. Bosworth RG, Birch EE. Nasal-temporal asymmetries in motion sensitivity and motion VEPs in normal infants and patients with infantile esotropia. *Am Assoc Pediatr Ophthalmol Strabismus Abst* 2003;38:61.
100. Naegele JR, Held R. The postnatal development of monocular optokinetic nystagmus in infants. *Vision Res* 1982;22:341-346.
101. Wattam-Bell J, Braddick O, Atkinson J, Day J. Measures of infant binocularity in a group at risk for strabismus. *Clin Vis Sci* 1987;4:327-336.
102. Jacobs M, Harris C, Taylor D. The development of eye movements in infancy. In: Lennerstrand G, ed. *Update on Strabismus and Pediatric Ophthalmology. Proceedings of the Joint ISA and AAPO&S Meeting. Vancouver, Canada. June 19 to 23, 1994*. Boca Raton, FL: CRC Press; 1994:140-143.
103. Tychsen L. Critical periods for development of visual acuity, depth perception and eye tracking. In: Bailey Jr DB, Bruer JT, Symons FJ, Lichtman JW, eds. *Critical Thinking About Critical Periods. National Center for Early Development and Learning, Univ North Carolina at Chapel Hill.* Baltimore, MD: Paul H. Brookes Publishing Co; 2001:67-80.
104. Schor CM, Levi DM. Disturbances of small-field horizontal and vertical optokinetic nystagmus in amblyopia. *Invest Ophthalmol Vis Sci* 1980;19:668-683.

105. Maurer D, Lewis TL, Brent HP. Peripheral vision and optokinetic nystagmus in children with unilateral congenital cataract. *Behav Brain Res* 1983;10:151-161.
106. Tychsen L, Hurtig RR, Scott WE. Pursuit is impaired but the vestibulo-ocular reflex is normal in infantile strabismus. *Arch Ophthalmol* 1985;103:536-539.
107. Tychsen L, Lisberger SG. Maldevelopment of visual motion processing in humans who had strabismus with onset in infancy. *J Neurosci* 1986;6:2495-2508.
108. Tychsen L, Rastelli A, Steinman S, Steinman B. Biases of motion perception revealed by reversing gratings in humans who had infantile-onset strabismus. *Dev Med Child Neurol* 1996;38:408-422.
109. Westall CA, Eizenman M, Kraft SP, Panton CM, Chatterjee S, Sigesmund D. Cortical binocularity and monocular optokinetic asymmetry in early-onset esotropia. *Invest Ophthalmol Vis Sci* 1998;39:1352-1360.
110. Tychsen L, Burkhalter A. Neuroanatomic abnormalities of primary visual cortex in macaque monkeys with infantile esotropia: preliminary results. *J Pediatr Ophthalmol Strabismus* 1995;32:323-328.
111. Chino Y, Smith EL, Hatta S, Cheng H. Suppressive binocular interactions in the primary visual cortex (V1) of infant rhesus monkeys. Presented at: Society for Neuroscience, 1996; Washington, DC.
112. Chino YM, Smith III EL, Hatta S, Cheng H. Postnatal development of binocular disparity sensitivity in neurons of the primate visual cortex. *J Neurosci* 1997;17:296-307.
113. Hatta S, Kumagami T, Qian J, Thornton M, Smith EL, Chino YM. Nasotemporal directional bias of V1 neurons in young infant monkeys. *Invest Ophthalmol Vis Sci* 1998;39:2259-2267.
114. Lowel S, Singer W. Selection of intrinsic horizontal connections in the visual cortex by correlated neuronal activity. *Science* 1992;255:209-212.
115. Löwel S, Engelmann R. Neuroanatomical and neurophysiological consequences of strabismus: changes in the structural and functional organization of the primary visual cortex in cats with alternating fixation and strabismic amblyopia. *Strabismus* 2002;10:95-105.
116. Trachtenberg JT, Stryker MP. Rapid anatomical plasticity of horizontal connections in the developing visual cortex. *J Neurosci* 2001;21:3476-3482.
117. Bailey P, von Bonin G. *The Isocortex of Man*. Urbana, IL: University of Illinois Press; 1951.
118. Volpe JJ. Hypoxic-ischemic encephalopathy: neuropathology and pathogenesis. *Neurology of the Newborn.* Vol 22. Philadelphia: WB Saunders; 1987:209-235.
119. Noetzel MJ, Brunstrom JE. The vulnerable oligodendrocyte. Inflammatory observations on a cause of cerebral palsy. *Neurology* 2001;56:1254-1255.
120. VanderVeen DK, Coats DK, Dobson V, et al. Prevalence and course of strabismus in the first year of life for infants with prethreshold retinopathy of prematurity. *Arch Ophthalmol* 2006;124:766-773.
121. Tychsen L, Burkhalter A. Nasotemporal asymmetries in V1: ocular dominance columns of infant, adult, and strabismic macaque monkeys. *J Comp Neurol* 1997;388:32-46.
122. Poggio GF, Gonzalez F, Krause F. Stereoscopic mechanisms in monkey visual cortex: binocular correlation and disparity selectivity. *J Neurosci* 1988;8:4531-4550.
123. Cumming BG, Parker AJ. Responses of primary visual cortical neurons to binocular disparity without depth perception. *Nature* 1997;389:280-283.
124. DeAngelis GC, Cumming BG, Newsome TW. Cortical area MT and the perception of stereoscopic depth. *Nature* 1998;394:677-680.
125. Cumming BG, DeAngelis GC. The physiology of stereopsis. *Annu Rev Neurosci* 2001;24:203-238.
126. Lund JS, Lund RD, Hendrickson AE, Bunt AH, Fuchs AF. The origin of efferent pathways from the primary visual cortex, area 17, of the macaque monkey as shown by retrograde transport of horseradish peroxidase. *J Comp Neurol* 1975;164:287-304.
127. Maunsell JHR, Van Essen DC. Functional properties of neurons in middle temporal visual area of the macaque monkey. II. Binocular interactions and sensitivity to binocular disparity. *J Neurophysiol* 1983;49:1148-1167.
128. Kawano K. Ocular tracking: behavior and neurophysiology. *Curr Opin Neurobiol* 1999;9:467-473.
129. Takemura A, Inoue Y, Kawano K, Quaia C, Miles FA. Single-unit activity in cortical area MST associated with disparity-vergence eye movements: evidence for population coding. *J Neurophysiol* 2001;85:2245-2266.
130. Livingstone MS, Hubel DH. Anatomy and physiology of a color system in the primate visual cortex. *J Neurosci* 1984a;4:309-356.
131. Malach R, Amir Y, Harel M, Grinvald A. Relationship between intrinsic connections and functional architecture revealed by optical imaging and *in vivo* targeted biocytin injections in primate striate cortex. *Proc Nat Acad Sci USA* 1993;90:10469-10473.
132. Dursteler MR, Wurtz RH, Newsome WT. Directional pursuit deficits following lesions of the foveal representation within the superior temporal sulcus of the macaque monkey. *J Neurophysiol* 1987;57:1262-1287.
133. Hoffmann K-P, Distler C. The optokinetic reflex in macaque monkeys with congenital strabismus. Presented at: IV Symposium of the Bielschowsky Society for the Study of Strabismus, 1992; Eye Clinic Heidelberg of the Ruprecht-Karls University, Germany.
134. Fuchs AF, Mustari MJ. The optokinetic response in primates and its possible neuronal substrate. In: Miles SA, Wallman J, eds. *Visual Motion and Its Role in the Stabilization of Gaze*. New York: Elsevier; 1993:343-369.

135. Kiorpes L, Walton PJ, O'Keefe LP, Movshon JA, Lisberger SG. Effects of artificial early-onset strabismus on pursuit eye movements and on neuronal responses in area MT of macaque monkeys. *J Neurosci* 1996;16:6537-6553.
136. Mustari MJ, Tusa RJ, Burrows AF, Fuchs AF, Livingston CA. Gaze stabilizing deficits and latent nystagmus in monkeys with early-onset visual deprivation: role of the pretectal NOT. *J Neurophysiol* 2001;86:662-675.
137. Dürsteler MR, Wurtz RH. Pursuit and optokinetic deficits following chemical lesions of cortical areas MT and MST. *J Neurophysiol* 1988;60:940-965.
138. Jampolsky A. When should one operate for congenital strabismus? In: Brockhurst RJ, Boruchoff SA, Hutchinson BT, Lessell S, eds. *Controversy in Ophthalmology*. Philadelphia: WB. Saunders; 1977:416-422.
139. von Noorden GK. *Binocular Vision and Ocular Motility: Theory and Management of Strabismus*. 5th ed. St Louis: CV Mosby; 1996.
140. The Early vs Late Infantile Strabismus Group. The early vs. late infantile strabismus surgery study: first monitoring report. *Strabismus* 1994;2:87-102.
141. Birch EE, Stager DR, Berry P, Everett ME. Prospective assessment of acuity and stereopsis in amblyopic infantile esotropes following early surgery. *Invest Ophthalmol Vis Sci* 1990;31:758-765.
142. Ing MR. Surgical alignment prior to six months of age for congenital esotropia. *Trans Am Ophthalmol Soc* 1995;93:135-146.
143. Birch E, Stager D, Wright K, Beck R, Pediatric Eye Disease Investigator Group. The natural history of infantile esotropia during the first six months of life. *J AAPOS* 1998;2:325-328.
144. Pediatric Eye Disease Investigator Group. Spontaneous resolution of early-onset esotropia: experience of the congenital esotropia observational study. *Am J Ophthalmol* 2002;133:109-118.
145. Fu VLN, Stager DR, Birch EE. Progression of intermittent, small angle, and variable infantile esotropia. *Invest Ophthalmol Vis Sci* 2007;48:661-664.
146. Ing MR, Okino LM. Outcome study of stereopsis in relation to duration of misalignment in congenital esotropia. *J AAPOS* 2002;6:3-8.